

**PERFORMANCE OF A CLOSED-LOOP INDUCTION MOTOR
SPEED CONTROL SYSTEM WITH
INTEGRAL-CYCLE-CONTROLLED SCR'S
IN ROTOR CIRCUIT**

A DISSERTATION

*Submitted in partial fulfilment of the
requirements for the award of the degree*

of

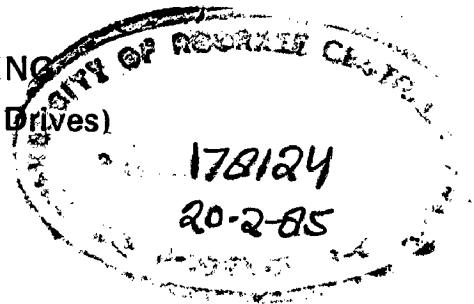
MASTER OF ENGINEERING

in

ELECTRICAL ENGINEERING

(Power Apparatus & Electric Drives)

**CHECKED
1995**



By

RAMESH CHAND



**DEPARTMENT OF ELECTRICAL ENGINEERING
UNIVERSITY OF ROORKEE
ROORKEE-247 667 (INDIA)**

January, 1985

C E R T I F I C A T E

Certified that the dissertation entitled " PERFORMANCE OF A CLOSED LOOP INDUCTION MOTOR SPEED CONTROL SYSTEM WITH INTEGRAL-CYCLE-CONTROLLED SCR'S IN ROTOR CIRCUIT ", which is being submitted by Sri RAMESH CHAND in partial fulfilment of the requirement for the award of the Degree of MASTER OF ENGINEERING IN ELECTRICAL ENGINEERING of University of Roorkee, Roorkee is a bonafide work carried out by him under our supervision and guidance. The matter embodied in this dissertation has not been submitted for the award of any Degree or Diploma.

It is further certified that he has worked for a period of about 11 months from January 1984 to December 1984 for preparing this dissertation at this University.

Bhim Singh
 7.1.85
 (BHIM SINGH)
 LECTURER
 ELECTRICAL ENGG. DEPTT.
 UNIVERSITY OF ROORKEE
 ROORKEE

R. B. Saxena
 (R. B. SAXENA)
 PROFESSOR
 ELECTRICAL ENGG. DEPTT.
 UNIVERSITY OF ROORKEE
 ROORKEE

ROORKEE
 DATED: JANUARY 7, 1985

A B S T R A C T

The closed-loop solid state resistance controller for a three phase slip ring induction motor has been designed fabricated and tested. The controller consists of two banks of three phase resistors, in the rotor circuit, one of them connected in series with the thyristors and another one in parallel with thyristors. The speed variation is obtained by varying the rotor resistance between R_{ON} and R_{OFF} by using integral cycle control. The various functional blocks which govern the behaviour of the system for small variations about the operating point are described. The responses for load and reference speed perturbations are obtained analytically. The analytical results are compared with the experimental values.

The same solid-state resistance controller has been modified to obtain optimum dc dynamic braking. The braking with slip-ring shorted, optimum resistance in the rotor circuit and with solid-state resistance controller are investigated. The braking performance characteristics have been obtained analytically for each of the above methods and compared with experimental results.

--

A C K N O W L E D G E M E N T

The author wishes to express his profound gratitude to Dr. R. B. Saxena, Professor in Electrical Engineering Department and Dr. Bhim Singh, Lecturer in Electrical Engineering Department for their able guidance and consistent encouragement, without which this work could not have been brought out in the present form.

The author is very much grateful to Dr. M. P. Dave, Professor and Head of Electrical Engineering Department for providing facilities to carry out the present work.

Last, but not the least, the author would like to thank the authorities of the Roorkee University Regional Computer Centre for permitting him to use the Computer facilities and Sri S. K. Banerjee, Research Technician and other P. G. Lab Staff for their assistance throughout the tenure of this work.

ROORKEE
DATED JANUARY 7, 1985


RAMESH CHAND

LIST OF SYMBOLS USED

SYMBOLS	DESCRIPTION
R_1	= Stator resistance / ϕ
X_1	= Stator reactance / ϕ
R_2	= Rotor resistance / ϕ
X_2	= Rotor reactance / ϕ
R_p	= Resistance in parallel with the thyristors / ϕ
R_s	= Resistance in series with the thyristors / ϕ
R_m, X_m	= Magnetising branch components of the machine.
R_t	= Equivalent rotor resistance of speed control Schemo / ϕ
R_t'	= Equivalent rotor resistance plus rotor resistance for dc dynamic braking / ϕ
α	= p.u. firing control delay.
V_R	= dc reference voltage
V_C	= Output Voltage of controller
m	= Slope of ramp voltage generated by ramp generator.
ω_r	= rotor speed in rad/sec.
V	= Voltage applied to the Stator of machine / ϕ (speed control scheme)
f	= Frequency of the voltage applied to the stator.
ω_{ro}	= Steady state rotor speed in rad/sec.
α_0	= p.u. firing delay at steady state speed.
I_s	= Stator current / ϕ

I_r	=	rotor current/ ϕ
E_o	=	Stator applied voltage of thevenin's equivalent circuit of machine.
S_r	=	Slip for closed loop ^{Speed} speed control.
ω_s	=	Synchronous speed of the machine.
I_d	=	Stator excitation for dc dynamic braking.
E	=	Air gap emf. at synchronous speed.
S_d	=	Slip for dc dynamic braking condition.
I_m	=	Resultant alternating current/ ϕ for braking.
E_{ro}	=	rotor emf at at synch speed for dc dynamic braking.
E_r	=	Rotor emf at other than synch speed.
ψ_2	=	Angle between E_r and I_r .
S_{cr}	=	Slip for which torque is maximum.
K_T	=	combined gain constant of techogenerator, rectifier and filter.
T_T	=	Effective time constant of filter.
K_C	=	Proportional gain constant of controller.
K_C/T_C	=	Integral gain constant of controller.
K_f	=	Gain constant of firing control circuit.

- T_f = Time constant of firing control circuit.
- T_d = Torque developed by the machine N -m.
- K_4, K_5 = Constants for the machine.
- K_M = Gain of constant of the mechanical system.
- T_M = Time constant of the mechanical system.
- F = Frictional constant of the rotating system in N-m/rad/sec..
- J = Moment of inertia of the rotating system in K g.-m²
- T_b = Braking torque in N-m.
- S_{ip} = Slip when braking starts.
- S_{fin} = final value of slip upto which braking resistance is effective.
- Δ = Small variation.

--

C O N T E N T S

<u>CHAPTER</u>		<u>PAGE Nos</u>
	C E R T I F I C A T E	-- (i)
	A C K N O W L E D G E M E N T S	-- (ii)
	A B S T R A C T	-- (iii)
	L I S T O F S Y M B L E S U S E D	-- (iv)
	C O N T E N T S	-- (vii)
1.	I N T R O D U C T I O N	-- 1- 4
2.	P R O P O S E D S C H E M E	-- - 5-24
	2-1 Principle of Operation	-- - 5
	(2-1-1) Closed Loop Speed Control Operation	- 5
	(2-1-2) FC Dynamic Braking Operation	- 7
	2-2 Description of System	-- - 8
	2-3 Design and Fabrication	-- - 11
	(2-3-1) Techogenerator, Rectifier and Filter	- 11
	(2-3-2) Controller	-- - 12
	(2-3-3) Firing Control Scheme	-- - 13
	(2-3-4) Induction Motor	-- - 18
3-	A n a l y s i s O F T H E S C H E M E - S P E E D C O N T R O L O P E R A T I O N s	- 25 -32
	3-1 Theory	-- - 25
	3-2 Dynamic Performance	-- - 30

(Continued ----)

C O N T E N T S

<u>CHAPTER</u>		<u>PAGE Nos.</u>
4-	ANALYSIS OF THE SCHEME - DC DYNAMIC BRAKING	33 -42
4-1	Theory --	33
5-	PERFORMANCE - CHARACTERISTICS --	43 -51
5-1	Computation of Characteristics and Their Experimental Verification	43
(5-1-1)	Computed Results --	45
(a)	Speed Control Scheme --	45
(b)	DC Dynamic Braking --	46
(5-1-2)	Experimental Results --	48
(a)	Speed Control Scheme --	48
(b)	DC Dynamic Braking --	49
5-2	Discussion of Results--	50
6-	CONCLUSIONS AND SUGGESTIONS FOR FURTHER WORK	52 -57
	BIBLIOGRAPHY --	55

APPENDIX 'A'	- SPECIFICATIONS AND PARAMETERS OF THE TEST MACHINE .	58
APPENDIX-'B'	- DEVELOPED COMPUTER PROGRAMME FOR SPEED CONTROL SCHEME	60
APPENDIX-'C'	- DEVELOPED COMPUTER PROGRAMME FOR DC DYNAMIC BRAKING	62

C O N T E N T S (continued...)

<u>CHAPTER</u>		<u>PAGE NOS</u>
TABLE-I	TORQUE V _s FIRING DURATION (α) FOR DIFFERENT ROTOR SPEEDS.	21
TABLE-II	TORQUE V _s SPEED FOR DIFFERENT VALUES OF SLIP	22
TABLE-III	VARIOUS GAIN AND TIME CONSTANTS USED FOR PERTURBATION STUDY	24
TABLE-IV	STOPPING TIME AND ENERGY LOSSES IN DC DYNAMIC BRAKING WITH AND WITHOUT SOLID STATE CONTROLLER;	47

CHAPTER - 1

INTRODUCTION

Induction motor is generally used as electric drive in many industry applications. The induction machine, often the best choice among ac machines for many industrial tasks, is simple, robust in construction, requires less maintenance and is the most suitable one in hostile environments. Its cost per KVA is much less than the dc machines. Conventionally, it could only be used as a constant speed drive. In some applications, it is desired to have a variable speed drive. The variable speed drive can also be achieved from induction machines. The basic well-known techniques through which efforts are made to obtain a suitable variable speed drive system are; stator voltage control method, stator voltage/current and frequency control method, rotor power control method and rotor resistance control method. With the advent of power semi-conductor technology, all these speed control techniques can be obtained electronically. For low and medium power slip-ring induction motors, the rotor resistance control method is simple and economical one. The rotor resistance control technique can provide high starting torque with low starting current. The speed of the motor can be varied over a wide range below synchronous speed. The power factor is generally improved by this method. Thus, this method of speed control is extensively used where a high

starting current may cause serious line disturbances or where intermittent starting is required which may require high starting torque.

In conventional methods, the rotor resistance may be varied manually in discrete steps. This mechanical operation for speed control is undesirable due to discontinuous speed variation and slow response. With the recent development in power semiconductor technology, these undesirable features of the conventional rheostatic control scheme can be eliminated and the smooth variation of speed is obtained. Attempts have been made recently to use SCR's (silicon controlled rectifiers) in different configurations in the rotor circuit [2, 5, 13- 15, 18, 20]. From which the continuous and contactless variation of rotor resistance is obtained. Most of these techniques uses SCR's in the rotor circuit, in phase controlled or chopper controlled mode. In phase controlled mode [2, 13, 14, 15] SCR's used in the rotor circuit, operates at slip frequency. The instant at which the current flow begins (in each half cycle) is obtained by controlling the angle of firing pulses to each SCR. Since the torque is developed only when the current flows through the rotor circuit, the control of the firing angle of SCR's controls the torque developed. Thus the average torque developed is controlled by controlling the firing angle of SCR's, and at a constant speed, the motor torque can be varied from minimum to maximum limit. But this scheme has certain limitations. It requires a complicated control circuitary as the rotor frequency changes with the change in rotor speed.

In chopper controlled mode [5, 18, 20], a three phase rectifier bridge is used in the rotor circuit. The rectified dc voltage is fed to the thyristor-chopper-controlled resistance. The effective rotor resistance is controlled by varying the duty cycle of the chopper. This scheme has limitations at low values of slip and employs forced commutation which involve additional commutating circuitry and an auxiliary voltage source. Thus both the schemes are uneconomical and do not fit for industrial drives.

Here a solid state resistance controller using inverse-parallel thyristors (or triacs) in the rotor circuit has been developed. The speed of the rotor can be varied at a fixed load torque. Likewise, the developed torque of the motor can be varied between a minimum to maximum value, at a constant value of speed. In the present scheme of speed control, the total effective resistance in the rotor circuit remains substantially high when the SCR's not in conducting mode and when the SCR's are in conducting mode, the effective rotor resistance becomes marginal. By controlling the ON time of SCR's in a closed loop manner a stepless control of rotor resistance is obtained and the speed of the motor can be controlled. The rotor speed is highest at minimum value of rotor resistance and varies to the lower value as the rotor resistance is increased. For braking mode of operation, the effective rotor resistance is varied in such a way that the peak braking torque is maintained throughout the speed range. This has been achieved by using the solid state resistance controller.

The dynamic behaviour [14] of the closed loop control scheme with solid state resistance controller in the rotor is investigated. The various functional blocks governing the behaviour of the system about the operating point has been described. The change in rotor speed with load and reference speed perturbations are obtained analytically. The analytical results are compared with the experimental observations. The steady state analysis of braking mode of operation (dc dynamic braking) [6] has been investigated. The investigation in this thesis deals with the braking performance of the slip ring induction motor in three operating modes -(i) with rotor slip rings short circuited (ii) with optimum resistance in the rotor circuit and (iii) with solid state resistance controller in the rotor circuit.

The braking performance is obtained in three different operating modes. With the present solid state controller, the braking performance is improved remarkably, in terms of stopping time as well as energy losses compared to the slip-ring shorted condition/^{and}with optimum resistance in the rotor circuit.

CHAPTER - 2

PROPOSED SCHEME

The first part of this chapter deals with the operating principle of the proposed scheme. Second part of this chapter gives description of the system. At last the design and fabrication of the system is investigated.

2-1 Principle of Operation:

The operating principle for both closed-loop speed control scheme and dc dynamic braking are as follows;

2.1.1 Closed-Loop Speed Control Operation:

The proposed solid-state rotor resistance controller comprises two sets of three identical resistors (Fig.2.1.1). Four SCR's TH_1 , TH_2 , TH_3 , & TH_4 are connected in two phases (using back to back connections) in one of the two sets of resistors. The resistance per phase, in series with SCR's is represented by R_s and in parallel with SCR's is represented by R_p .

Thyristors are triggered by incorporating triggering pulses at the gates. The periodic wave form of triggering pulses used in the present scheme are shown in Fig.2.1.2. These wave forms are generated by a suitable controller circuit to trigger the thyristors. The triggering pulses gets thyristors in ON state for both positive and negative half cycles in each of the two phases as these are used in pair for each phase with reverse connections. Third phase is directly connected to form star connection. The period T is the ON plus OFF period of thyristors and is represen-

ted by one cycle. The time period T is chosen on mechanical considerations of the test machine. The parameters of the mechanical system of the machine are to be such that the effect on the speed due to torque pulsations of frequency $1/T$ could be sufficiently damped. T is roughly chosen about four times the period corresponding to the lowest slip frequency and at the same time about $\frac{1}{4}$ th of the mechanical time constant of the rotating system. The ON period T_{ON} can be varied from zero to T . When thyristors are in OFF state, the effective rotor circuit resistance per phase may be represented as -

$$R_{OFF} = R_p \quad \text{----} \quad (2.1.1)$$

and when thyristors are in ON state, the effective rotor resistance per phase will be -

$$R_{ON} = \frac{R_p \cdot R_s}{R_p + R_s} \quad \text{---} \quad (2.1.2)$$

Thus, the effective rotor resistance can be varied between R_{ON} and R_{OFF} by varying the ON period of thyristors.

The typical torque (VS) speed characteristics of the test machine with rotor resistance per phase R_{OFF} and R_{ON} , are given in fig.2.1.3. It is clear that for a certain load torque T_L , the steady state operating point is either at A; when thyristors are in OFF state or at B; when thyristors are in ON state. Thus by varying the ON state of thyristors, any intermediate value between A and B can be obtained. Therefore, for a constant load torque, the speed of the motor may be varied

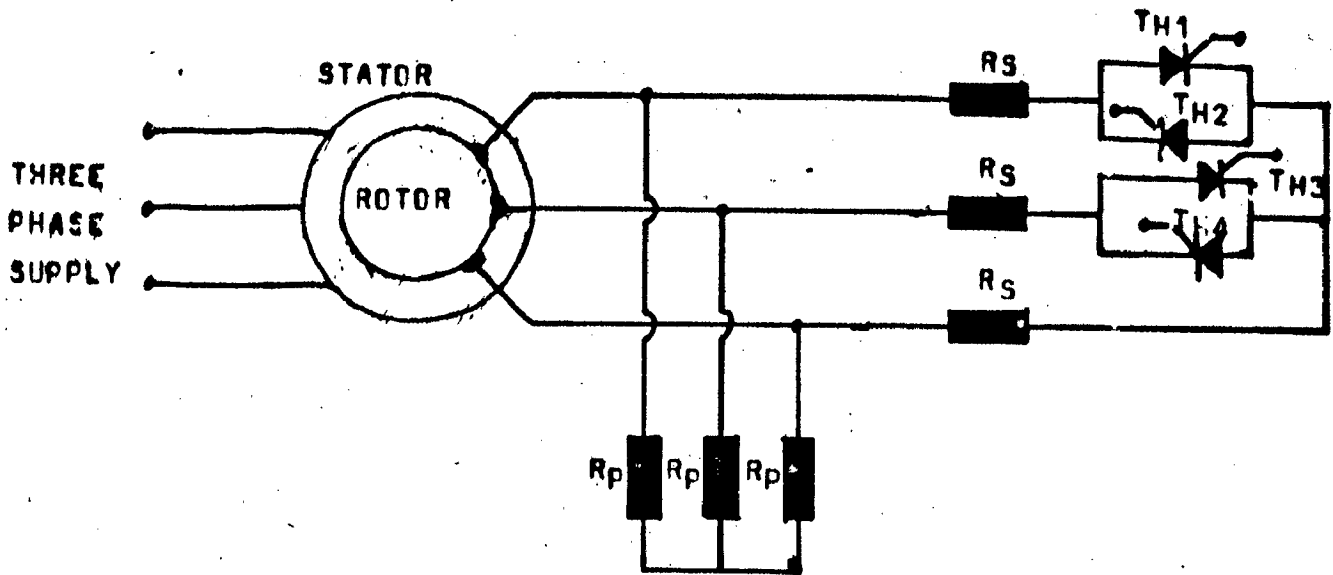


FIG.2.1.1 Schematic Diagram Of The Scheme

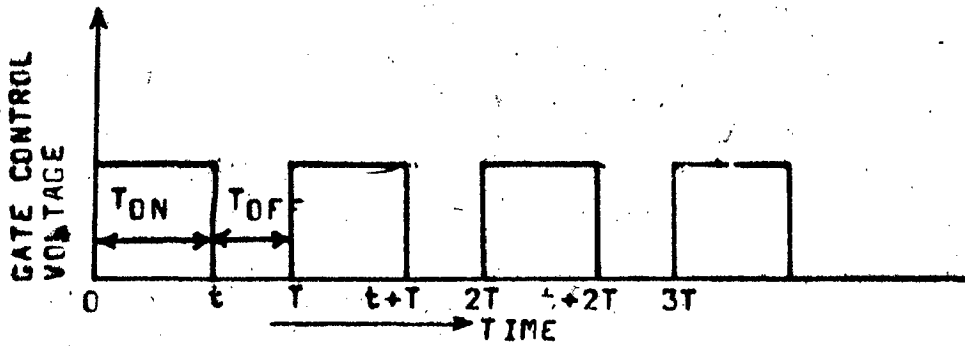


FIG.2.1.2 Gate Triggering Pulses

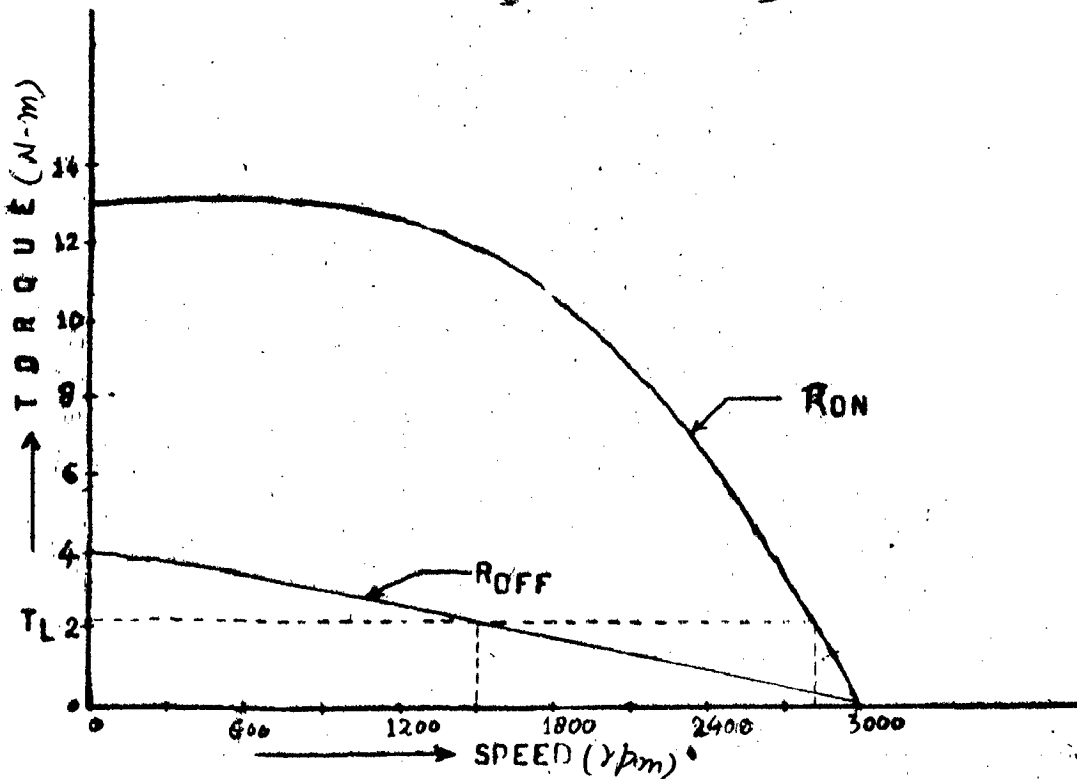


FIG.2.1.3 Typical Torque VS Speed Characteristics Of The Set

between A and B, by varying the rotor resistance between R_{OFF} and R_{ON} values.

The values R_p and R_s depends upon the speed range required. The minimum operating speed depends upon the maximum value of R_{OFF} and the maximum operating speed may be obtained from the value of R_{ON} . The value of current flowing through the thyristors depends upon the relative values of R_p and R_s . The thyristors are switched OFF at the current zero by natural commutation.

2.1.2 DC Dynamic Braking Operation:

For dynamic or rheostatic braking, the stator winding is used as a dc field winding and the rotor winding as an armature winding. With the present slip-ring machine, external resistance may be connected into the rotor circuit, to provide a resistive load. The stator winding of the machine is excited with dc supply voltage, in a number of ways.

The present solid state controller for dc dynamic braking also comprises two sets of three phase resistors bank as shown in Fig.2.1.4. Same firing control circuit is used except the controller design. The typical braking torque (VS) rotor speed curves are given ⁱⁿ Fig.2.1.5. From which it is clear that for getting peak braking torque, thyristors should be in OFF state at starting the braking. It is also clear that the braking time is optimum with solid state controller compared with slip-ring shorted and optimum resistance conditions.

During dynamic braking, the machine operates as a non-salient pole synchronous generator, loaded on to a bank of

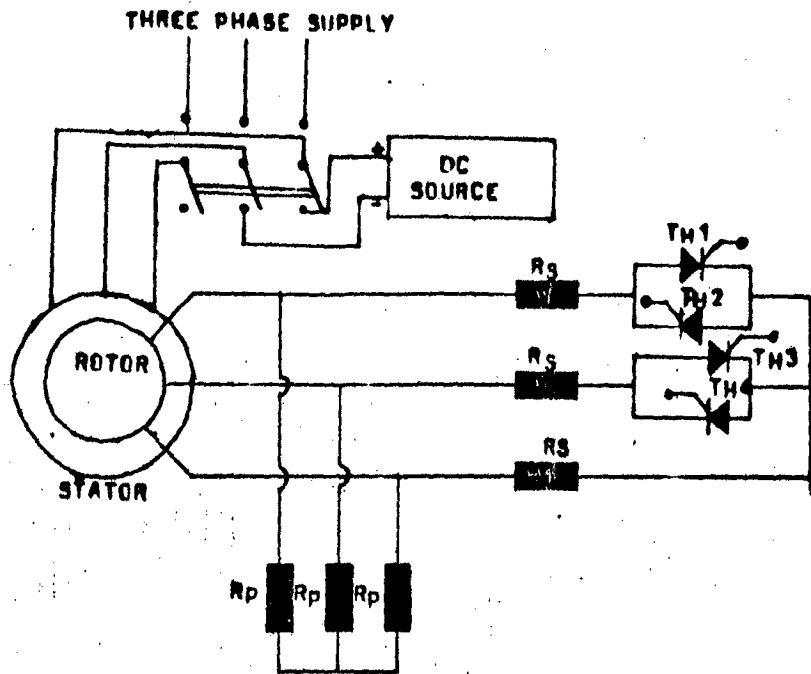


FIG. 2.1.4 SCHEMATIC DIAGRAM FOR DC DYNAMIC BRAKING WITH SOLID STATE CONTROLLERS

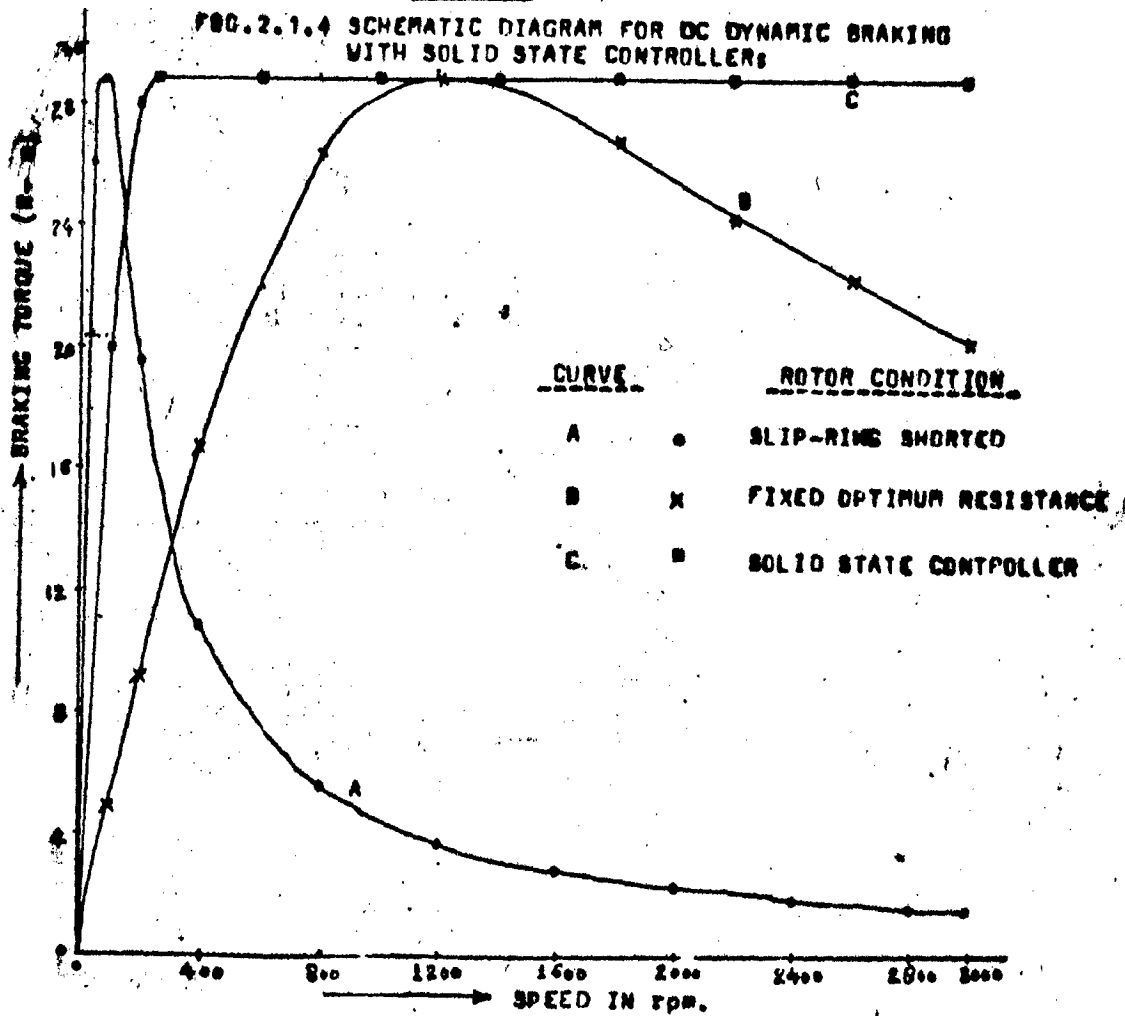


Fig 2.1.5 VARIATION OF BRAKING TORQUE WITH SPEED FOR SLIP-RING SHORTED, FIXED OPTIMUM RESISTANCE AND SOLID STATE CONTROLLER CASES, $I_s = 0.8 p.u.$

three phase resistors in the rotor. Although its speed changes, (decrease) with time, the frequency of the generated power also changes in proportion. The operating flux will vary widely with speed, e.g. at stand still, the whole of the exciting current is magnetising in nature, since there is no armature current at standstill.

2.2 Description of System:

The system considered here consists a slip ring induction motor. The two sets of three phase external resistors are connected through slip-rings of the test machine (Fig.2.1.1). Four thyristors are connected in two phases in series with one bank of resistors. A permanent magnet tachogenerator is mounted on the shaft of the motor. The tachogenerator generates an ac signal which is directly proportional to the speed of the rotor. The block diagram of the proposed scheme using feed back loop is shown in Fig.2.2.1. The ac signal voltage obtained from the tachogenerator output terminals is rectified to get a proportional dc voltage, using bridge rectifier. This dc voltage signal is first compared with a fixed reference voltage and then is applied to the controller. The error signal voltage is amplified in a desired manner by the controller. The stator terminals of the test machine are connected to the constant voltage and constant frequency three-phase supply. The rotor speed is adjusted with the variation of ON period of thyristors. The ON period of the thyristors may be represented in terms of p.u. firing delay (α) and now instead of using T_{ON}

we will use α where-ever necessary. The p.u.firing delay (α) may be defined as follows;

$$\alpha = \frac{T_{OFF}}{T_{ON} + T_{OFF}} \quad \text{---} \quad (2.2.1)$$

where T_{OFF} is the OFF period of thyristors.

and T_{ON} is the ON period of thyristors.

The dc reference voltage V_R compared with rectified techo-generator output voltage represents a set speed of the machine. The controller amplifies the so produced error voltage in a desired manner. The controller used may be mainly of three types:

- (a) Proportional (P) Controller.
- (b) Proportional plus integral (PI) controller.
- (c) Proportional plus integral plus derivative (PID) Controller.

P and PI controllers are considered for the present study. The function of controller is to give the required control voltage level in a desired manner, which in turn adjusts the firing duration (α) to a suitable value.

The dc dynamic braking (Chapter-1) may be obtained with rotor slip-rings short circuited and exciting the stator winding with d.c. supply. The stopping time of rotor ^{is} improved than the normal stopping of the motor. If we connect ^{an} external resistance in the rotor circuit and adjust it to such a value so that the stopping time of the rotor gets minimum - is called braking with optimum resistance connected to the rotor. In

braking with optimum resistance, the stopping time is improved than with rotor short-circuited. For achieving further improvement in stopping time, the solid state resistance controller is used. The value of R_p is kept sufficiently high when the braking is started (at highest possible speed of the rotor), so that the peak braking torque is obtained at highest speed. To do so, the thyristors are kept in OFF state when the braking is started. Again, as the motor speed slows down, the thyristors start conducting with gradually increased ON time and the effective rotor resistance decreases. The reduction in the rotor resistance is such that the peak braking torque is maintained throughout the speed range. The thyristors will be in ON state ($\alpha = 0$) before the speed gets to be zero. This is because that the rotor resistance cannot be decreased further than R_{0N} . Ofcourse R_{0N} is marginal due to the parallel combinations of R_p and R_s .

The schematic diagram for dc dynamic braking with solid state resistance controller is given in Fig.2.1.4. The typical braking torque (VS) speed characteristics for all the three conditions, viz; with slip-ring short circuited, with optimum resistance in the rotor circuit and with solid state resistance controller are shown in Fig.2.1.5. The stator excitation is taken 0.8 p.u. of the rated capacity.

Design and Fabrication:

A solid state resistance controller has been designed and simulated for the proposed closed loop operation. Also the controller for dc dynamic braking has been developed. The transfer functions for the various functional blocks of the feed-back system are given in the following sections:

Tachogenerator, Rectifier and Filter:

A permanent magnet tachogenerator is mounted on the same shaft of the test machine. The output voltage of tachogenerator is proportional to the shaft speed is ac in nature and is followed by a rectification and filtration before comparing with reference voltage V_R . Bridge rectifier using four semiconductor diodes is used for full wave rectification. The functional block diagram of tachogenerator, rectifier and filter is shown in as block B_1 (Fig.2.3.1). The transfer function of the block is represented as -

$$(s) = \frac{K_T}{(1+sT_T)} \quad \text{---} \quad (2.3.1)$$

where K_T is the combined gain constant of tachogenerator, rectifier and filter, and T_T is the effective time constant of the filter. The circuit configuration of rectifier with filter is given in Fig. 2.3.2.

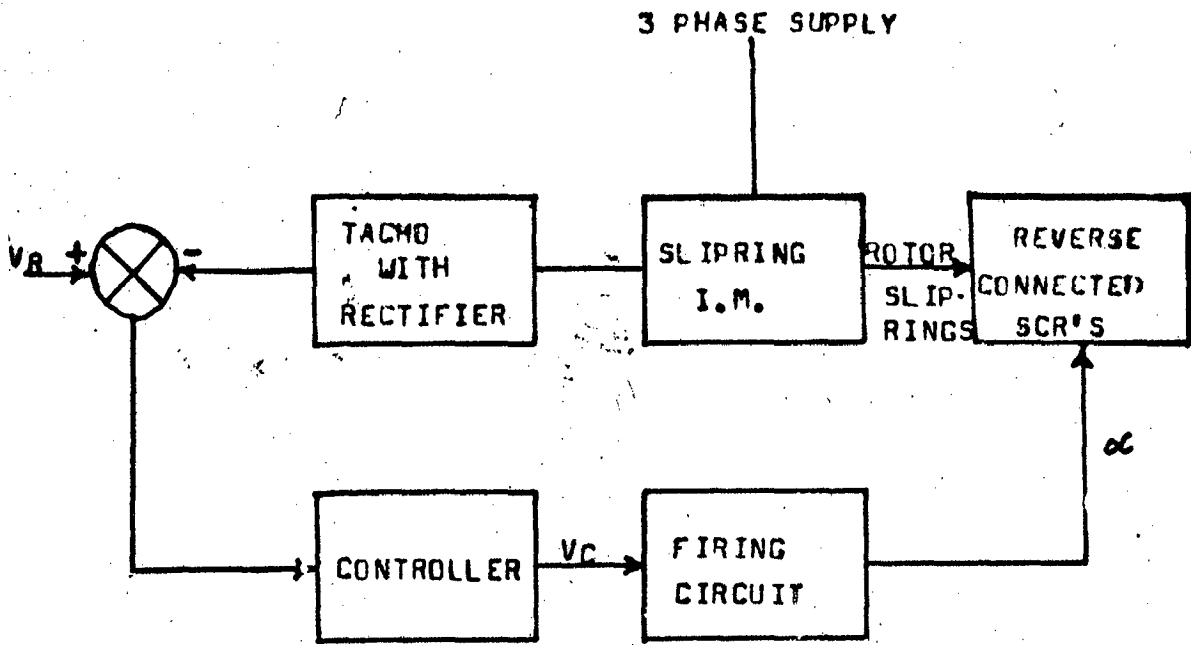


FIG 22.1 BLOCK DIAGRAM OF CLOSED-LOOP SYSTEM

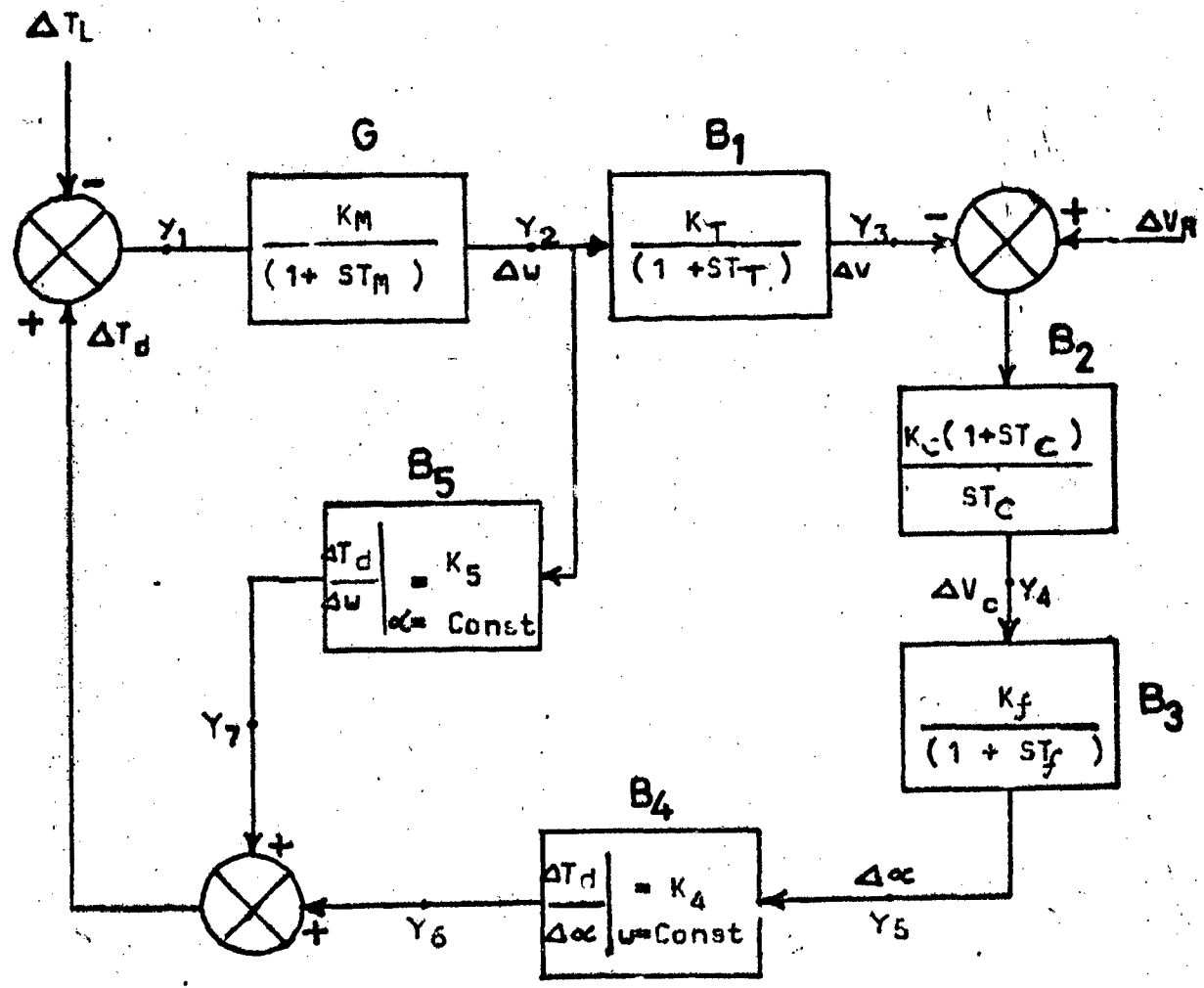


FIG 23.1 FUNCTIONAL BLOCKS OF CLOSED LOOP SYSTEM

2.3.2 Controller:

Controller is a device consisting of an amplifier and a power stage. The error signal voltage is given to the inverting terminal of an OP - AMP. The non-inverting terminal is grounded through a high resistance. A feedback signal is given to the same inverting point via an impedance. The nature of the impedance depends upon the manner desired by the controller, e.g.; it consists a pure resistance in the feedback loop for proportional amplification and combination of resistance and capacitance for proportional plus integral operation. The controller output voltage is corrected in accordance with the input change in voltage (error signal voltage). The controller is represented by Block B₂ in Fig. 2.3.1. The output voltage of controller is denoted by V_C. In the present work, proportional (P) and proportional plus integral (PI) controllers have been considered. The transfer functions for both the controllers are represented as follows;

(a) Proportional (P) Controller;

The transfer function of proportion controller is represented as;

$$G_C(s) = K_C \quad \text{---} \quad (2.3.2)$$

where K_C is the proportional gain constant of the controller.

(b) Proportional plus Integral (PI) Controller;

The transfer function of PI controller is represented as;

$$G_C(s) = \frac{K_C(1 + sT_C)}{s T_C} \quad \text{--- (2.3.3)}$$

where K_C is the proportional gain constant and K_C/T_C is the integral gain constant of the controller.

The circuit configurations of these two controllers are given in Fig.2.3.3.

The controller used for dc dynamic braking is a proportional one and the same is given in Fig.2.3.3.

2.3.3 Firing Control Scheme;

Firing pulses are required to turn ON the thyristors for a time duration T_{ON} . Thyristors remains in OFF state for the duration T_{OFF} i.e. $(T - T_{ON})$. T_{ON} may be varied from zero to T . When T_{ON} is equal to T , thyristors are in ON state for full duration T , and when T_{ON} is equal to zero, thyristors are in OFF state. The ON period of thyristors may be varied smoothly and linearly by varying a control voltage V_R from zero to its peak designed value. The complete firing control scheme is given in Fig. 2.3.4. Block B_3 in Fig.2.3.1 represents the functional block of firing control scheme. The change in firing duration (α) takes place in accordance with the change in control voltage V_C . The main parts of the firing control scheme are as follows;

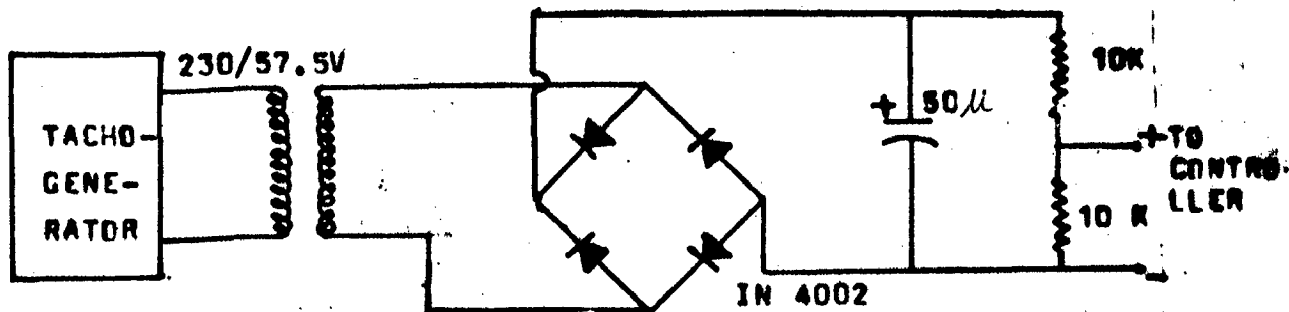
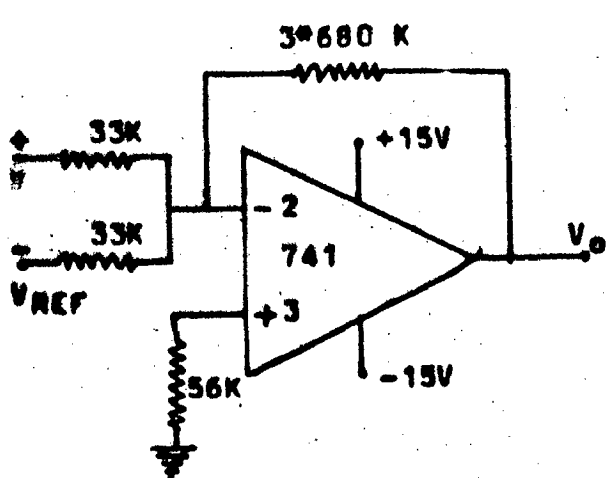
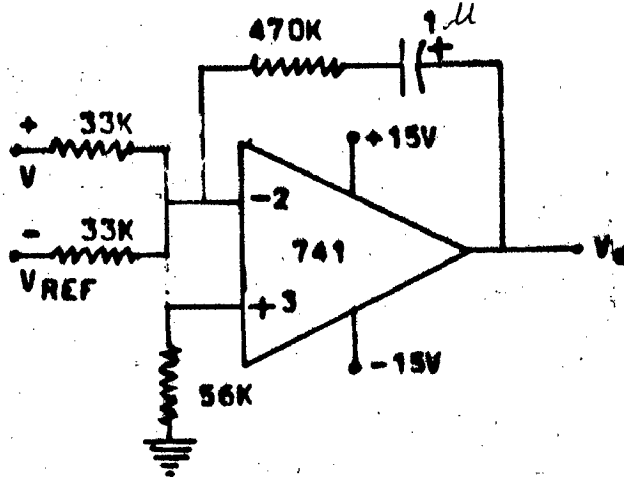


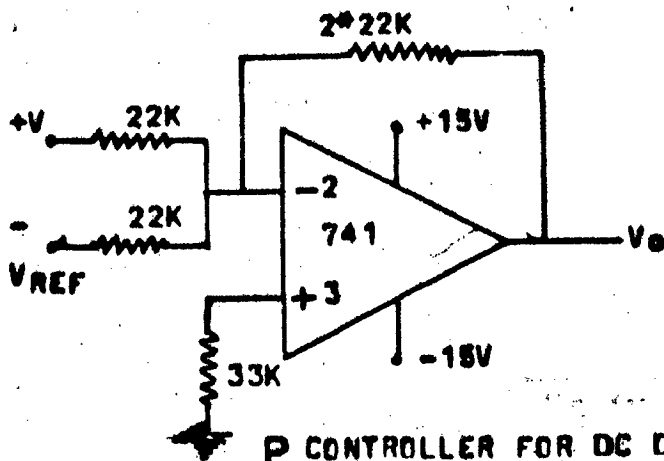
FIG. 2.3.2 CIRCUIT CONFIGURATIONS OF RECTIFIER AND FILTER



P CONTROLLER FOR SPEED CONTROL



PI CONTROLLER FOR SPEED CONTROL



P CONTROLLER FOR DC DYNAMIC BRAKING

FIG. 2.3.3 CIRCUIT CONFIGURATIONS OF CONTROLLERS

- (a) Low frequency oscillator
- (b) Ramp generator
- (c) Voltage comparator
- (d) High frequency oscillator
- (e) AND gating
- (f) Pulse amplifiers.

The wave-forms at the various points of the firing control diagram are given in Fig.2.3.5.

For a small change in V_c , the change in p.u. firing delay may be given as -

$$\Delta\alpha = \frac{1}{m} \cdot V_c \quad \text{--- (2.3.4)}$$

where m is the slope of the ramp voltage generated by ramp generator. All the parts of complete firing control scheme represented by blocks in Fig.2.3.4 are discussed in detail in the following paragraphs;

(a) Low Frequency Oscillator:

The circuit diagram for the low frequency oscillator is given in Fig.2.3.6. A 555 IC timer generates approximately square wave of low frequency. The timer is used here as an astable-multivibrator. The frequency of the generated wave may be calculated by using the ~~equation~~ equation given below;

$$f = \frac{1.44}{(R_A + 2R_B) C_T} \text{ Hz} \quad \text{--- (2.3.5)}$$

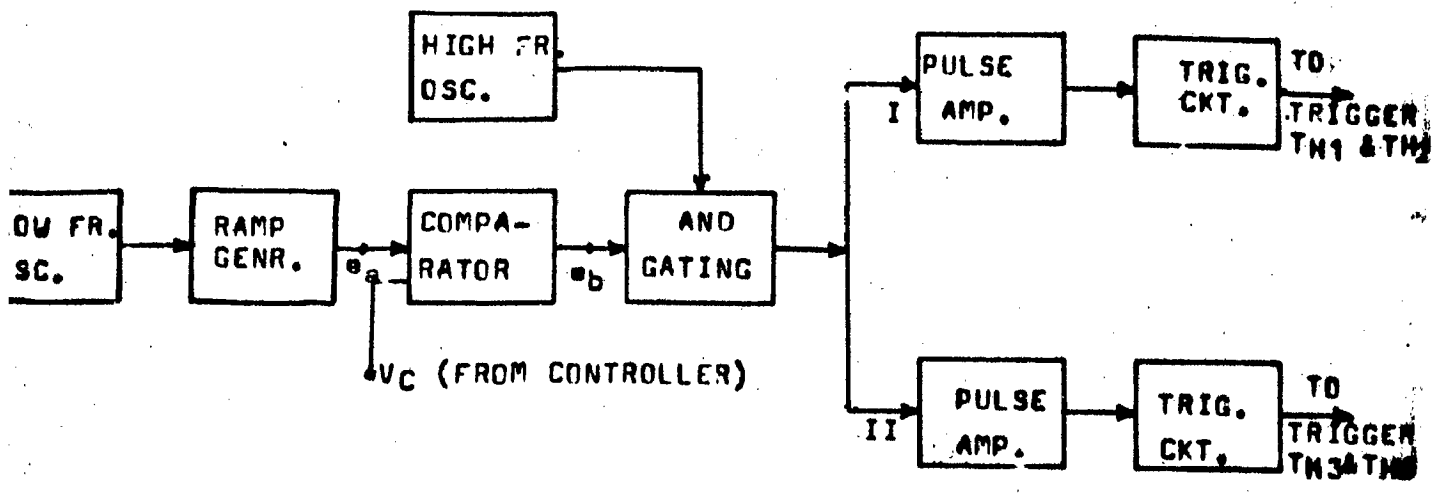


FIG.2.3.4 COMPLETE FIRING CONTROL SCHEME

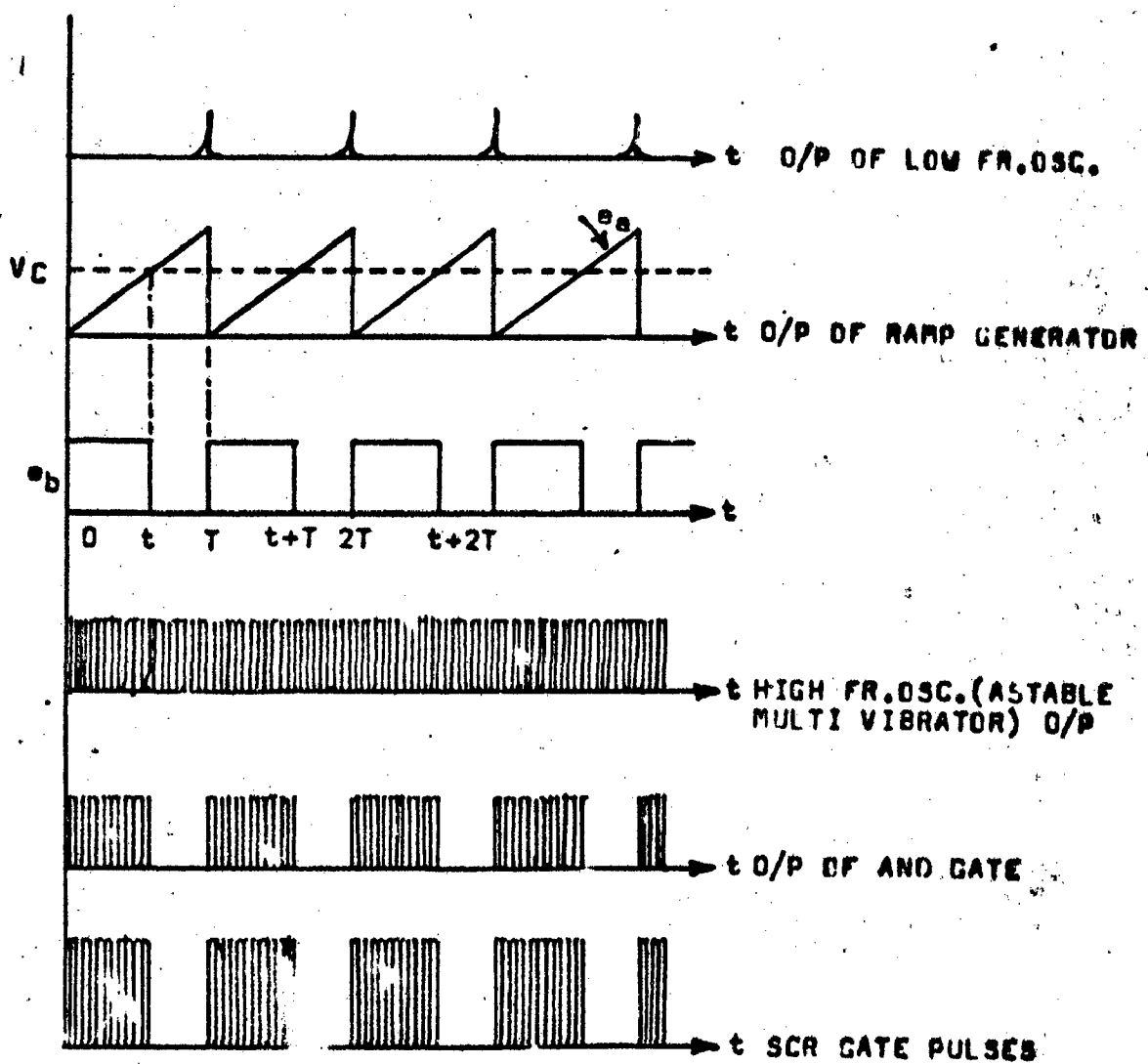


FIG.2.3.5 WAVEFORMS AT DIFFERENT POINTS

From the design values of R_A , R_B and C_T , the frequency of oscillation is calculated as 2Hz (approximately). V_{CC} may be varied from 5 to 15 volts, but here V_{CC} is fixed at 14 volts.

The low frequency (2Hz) square wave is differentiated by using R - C circuit, shown in Fig.2.3.6 capacitor C_1 charges and discharges through R_1 from the input signal and forms both positive and negative pulses in each cycle of input wave.

(b) Ramp Generator:

The circuit configuration of a simple ramp generator is given in Fig.2.3.7. Here the principle of constant current source is used. The capacitor C_2 is allowed to charge through a constant current source, comprising of T_1 , R_1 , R_2 , R_3 and R_4 . The constant current flows through C_2 and charges it linearly and isolates from the timing circuit through an ^{emitter} follower buffer stage T_2 . The differentiated (low frequency) pulses are given at the gate of n-p-n transistor T_2 . The transistor turns ON only for positive input pulses. Initially C_2 charges through constant current source. As positive pulse appears at the gate of transistor T_2 , it gets ON and C_2 gets discharged through it. Thus, a ramp voltage is obtained across the capacitor C_2 which is of the same frequency as the low frequency pulse input to it. From the design values, height of the ramp is about + 12 volt.

(c) Voltage Comparator;

The operational amplifier 741 I.C. is used as a voltage comparator. It is shown in Fig. 2.3.8. The ramp voltage signal is given at the inverting terminal and the control voltage V_c (the output of controller) is given at the non-inverting terminal of the OP-AMP. A dual supply ± 15 volt dc is given at pin No. 7 and 4; shown in Fig. 2.3.8. The comparator compares the ramp voltage with the control voltage V_c continuously. As the controller output voltage V_c varies from zero to its maximum limit (12 volt for the present case), the width of the comparator's output wave varies from zero to T .

(d) High Frequency Oscillator;

The 555 IC timer is used as a high frequency Oscillator. It is as shown in Fig. 2.3.9. The design parameters of R_A , R_B , and C_T gives the high frequency of oscillation (10 KHz approximately). The output waveform is approximately a square wave.

(e) And Gating with High Frequency Pulses;

The control voltage signal (output of the voltage comparator) is AND GATED with the high frequency pulses obtained from the high frequency oscillator. A simple AND GATING circuit diagram is shown in Fig. 2.3.10.

There are certain advantages of AND GATING the control signal with the high frequency waves. Few of them are as

follows:-

- 1) Only one astable multivibrator may be used for AND GATING with different control signals.
- 2) The scheme is suitable for sustained triggering of SCR's for a longer duration.
- 3) The size of the required pulse transformer is small.
- 4) The power dissipation in the SCR's gate is less compared with continuous sustained triggering and it may be adjusted to a minimum value.
- 5) Wide variation of the gate resistance does not affect the turning ON Operation of SCR's.

(f) Pulse Amplifier;

A two stage transistor amplifier has been used to amplify the pulse height obtainable from the AND GATING stage. Circuit configuration for the same is given in Fig.2.3.11.

Here power transistor SL-100 has been used for the first stage amplification. The transistor T_3 turns ON when an input positive pulse appears at the base of it (after AND GATING). The emitter current of T_3 is the first stage amplified gain.

This emitter current of T_3 is applied at the base of transistor T_4 to turn ON the same, which in turn gives the amplified current pulse appearing at the emitter of power transistor T_4 . These amplified pulses are applied to the primary winding of a pulse transformer. Secondary voltage of the pulse transformer

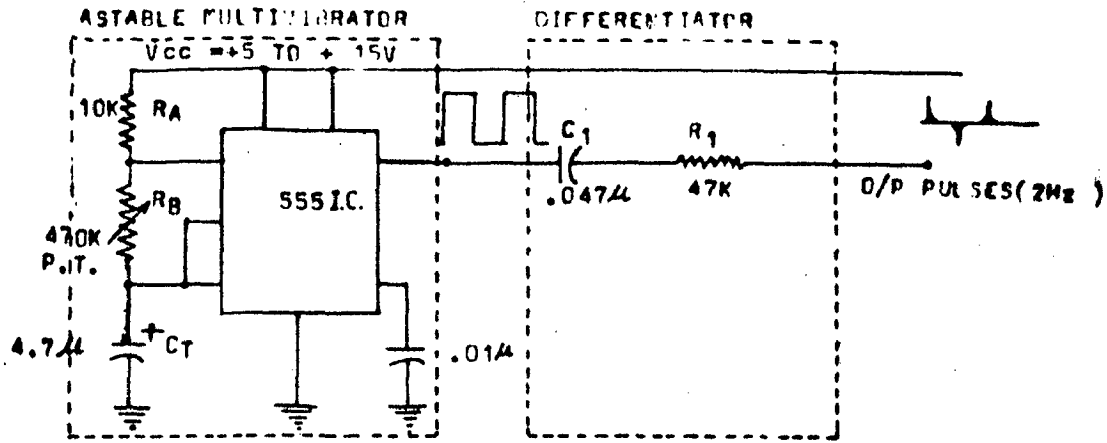


FIG.2.3.6 LOW FREQUENCY OSCILLATOR

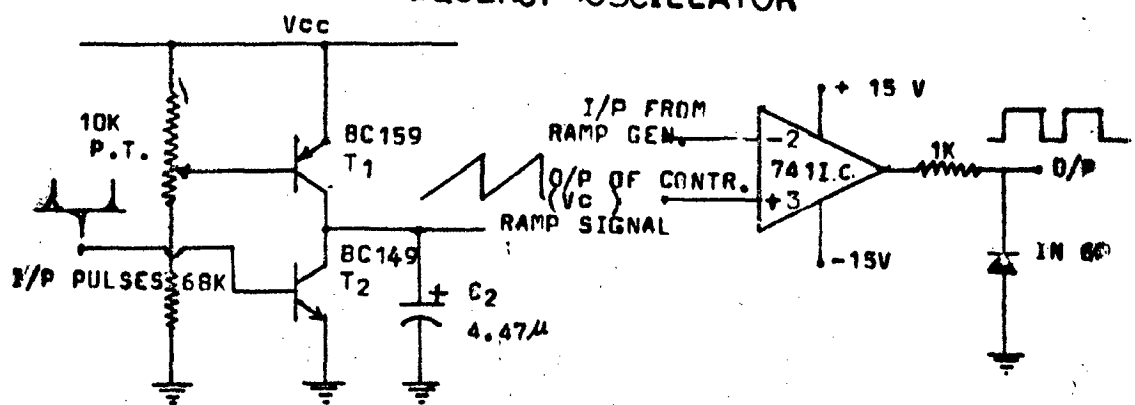


FIG.2.3.7 RAMP GENERATOR

FIG.2.3.8 VOLTAGE COMPARATOR

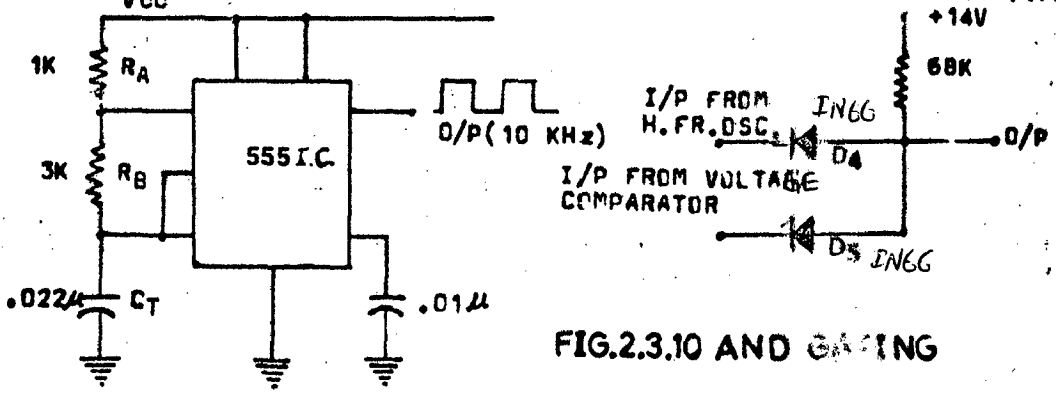


FIG.2.3.9 HIGH FREQUENCY OSC.

FIG.2.3.10 AND GATING

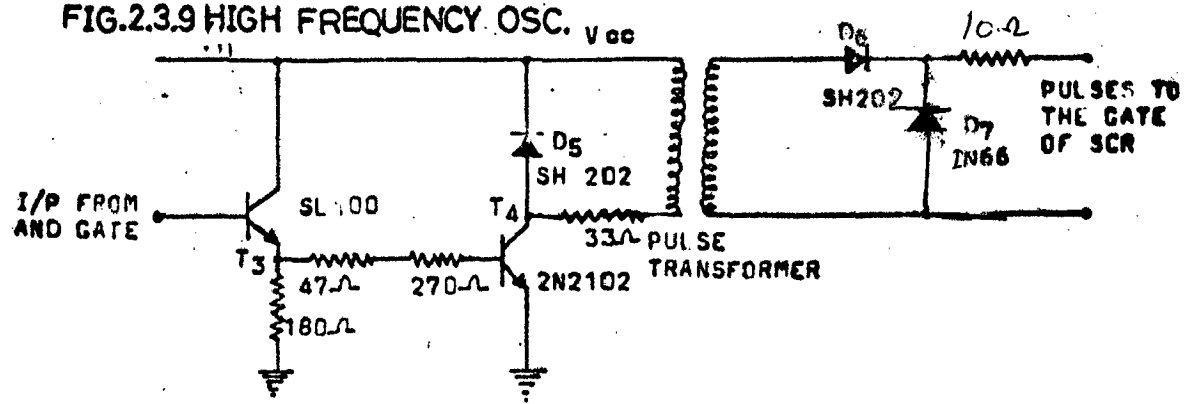


FIG.2.3.11 PULSE AMPLIFIER

is applied (through the protecting circuit) to the gate of SCR's. The use of pulse transformer is to get isolate the control circuit from the power circuit. Diode D₆ has been used to protect the transistor T₄ from the reverse biasing. Diodes D₇ and D₈ has been used to prevent the damage of the gates of SCR's due to negative spikes. The complete firing control circuit configuration is given in Fig. 2.3.12.

Although the comparator adjusts the ON period of thyristors to the new value as the change in V_c occurs, but the thyristors may not respond immediately. Here all the thyristors are triggered simultaneously. Thus atleast two separate units are required for triggering all the four thyristors from the isolation point of view.

The functional block for the firing control system is given in Fig.2.3.1, as block B₃. It is assumed that block B₃ is a first order system with gain constant K_f equal to 1/m and the time constant T_f. The transfer function of block B₃ may now be written as;

$$G_f(s) = \frac{K_f}{(1 + sT_f)} \quad \text{---} \quad (2.3.6)$$

2.3.4 Induction Motor;

The torque developed by the test machine at a given operating point is a function of speed of the machine, p.u.firing delay \propto

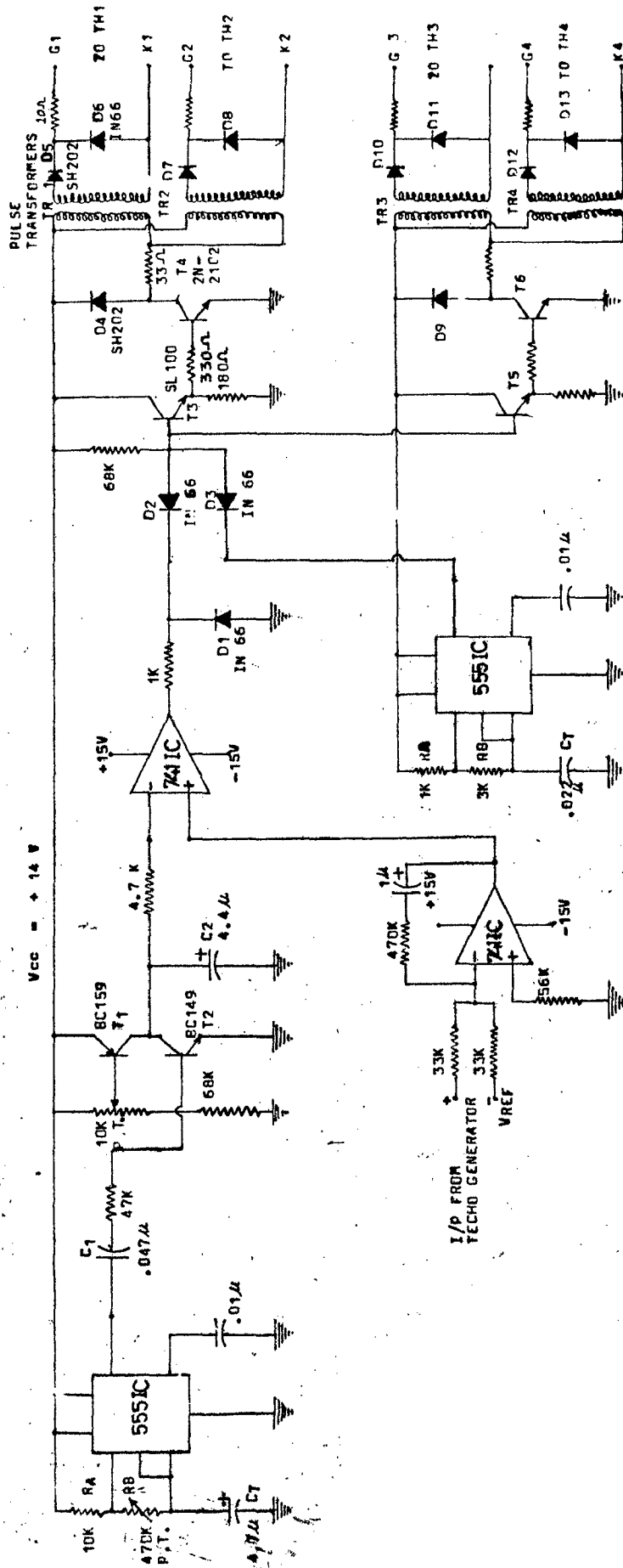


FIG.2.3.12 COMPLETE FIRING CONTROL SCHEME

of thyristors, voltage and frequency of the power supplied to the stator of the machine. The difference between developed torque and the load torque of the machine is the effective torque working on the rotating system. The developed torque dependent on the above variables may be represented in equation form-

$$T_d = F(\omega_r, \alpha, V, f) \quad \text{----} \quad (2.3.7)$$

where ω_r = rotor speed in rad/sec.

and α = per unit firing delay of thyristors.

To study the dynamic behaviour of the machine about its operating point, the reference voltage and developed torque has been perturbed. The small variation in developed torque may be expressed in terms of the small change in rotor speed and the firing delay as follows;

$$\Delta T_d = \left. \frac{\Delta T_d}{\Delta \alpha} \right|_{\omega_r = \text{const.}} \cdot \Delta \alpha + \left. \frac{\Delta T_d}{\Delta \omega_r} \right|_{\alpha = \text{const.}} \cdot \Delta \omega_r \quad \text{----} \quad (2.3.8)$$

This can be further expressed as,

$$\Delta T_d = K_4 \cdot \Delta \alpha + K_5 \cdot \Delta \omega_r \quad \text{---} \quad (2.3.9)$$

Where K_4 and K_5 are treated as constants for the machine which depend upon the operating point and may be obtained from the steady-state characteristics of the machine. The speed torque characteristics for different values of firing delay,

has been obtained from the equivalent circuit model of the slip ring induction motor (Chapter- 3). The variation of the developed torque with firing delay (α) for different values of rotor speed has also been plotted. The torque (V_s) firing delay curves at different values of speed are obtained and are shown in Fig.(2.3.13) Also the same are tabulated in Table No.I. The torque (V_s) rotor speed curves are shown in fig.2.3.14 and are tabulated in Table No.II.

The steady state values of firing delay and the rotor speed may be taken as α_0 and ω_{r0} respectively. The constant K_4 which is defined as the ratio of ΔT_d and $\Delta \alpha$ with speed constant (eqn.2.3.8) is the slope of torque (V_s) firing delay curve at the operating point (ω_{r0}, α_0). This has been obtained from the curves given in Fig.2.3.13. Also the constant K_5 which is defined as the ratio of ΔT_d and $\Delta \omega_r$ with the constant value of α , is the slope of torque (V_s) slip graph at the same operating point. Constant K_5 has been obtained from the curves given in Fig.(2.3.14).

Now the values of K_4 and K_5 have been obtained from the results of steady state analysis and these values have been used for the present perturbation study. The resultant change in the developed torque may be expressed, as the summation of $K_4 \cdot \Delta \alpha$ and $K_5 \cdot \Delta \omega_r$ which are the outputs of blocks B_4 and B_5 respectively (Fig.2.3.1). The change in the developed torque is compared with the change in load torque. The resultant torque

T A B L E - ITORQUE VS FIRING DURATION (α) FOR DIFFERENT
ROTOR SPEED

FIRING DURATION (α)	TORQUE (N-m) FOR					
	SLIP= 1.0	SLIP=.8	SLIP=.6	SLIP= .3	SLIP=0.2	SLIP= 0.1
0.0	15.07	13.69	11.63	6.91	4.85	2.54
0.1	14.68	13.22	11.13	6.52	4.56	2.38
0.2	14.20	12.67	10.56	6.10	4.25	2.21
0.3	13.60	12.01	9.60	5.64	3.91	2.03
0.4	12.86	11.23	9.15	5.13	3.54	1.83
0.5	11.93	10.29	8.29	4.57	3.14	1.61
0.6	10.76	9.16	7.29	3.96	2.70	1.38
0.7	9.30	7.81	6.14	3.27	2.22	1.13
0.8	7.45	6.18	4.79	2.51	1.70	0.86
0.9	5.14	4.20	3.22	1.65	1.11	0.56
0.97	3.29	2.67	2.02	1.03	0.69	0.35

TABLE - IITORQUE Vs SPEED FOR DIFFERENT VALUES OF α

SLIP	TORQUE (N-m) FOR				
	$\alpha = 0.0$	$\alpha = 0.3$	$\alpha = 0.5$	$\alpha = 0.72$	$\alpha = 0.85$
0.1	2.54	2.03	7.61	1.09	0.71
0.2	4.85	3.91	3.14	2.14	1.41
0.3	6.91	5.64	4.57	3.15	2.09
0.4	8.72	7.22	5.91	4.12	2.76
0.5	10.29	8.64	7.15	5.04	3.41
0.6	11.63	9.90	8.29	5.55	4.03
0.7	12.76	11.03	9.34	6.80	4.64
0.8	13.69	12.01	10.29	7.60	5.23
0.9	14.46	12.87	11.15	8.30	5.81
1.0	15.07	13.60	11.93	9.02	6.36

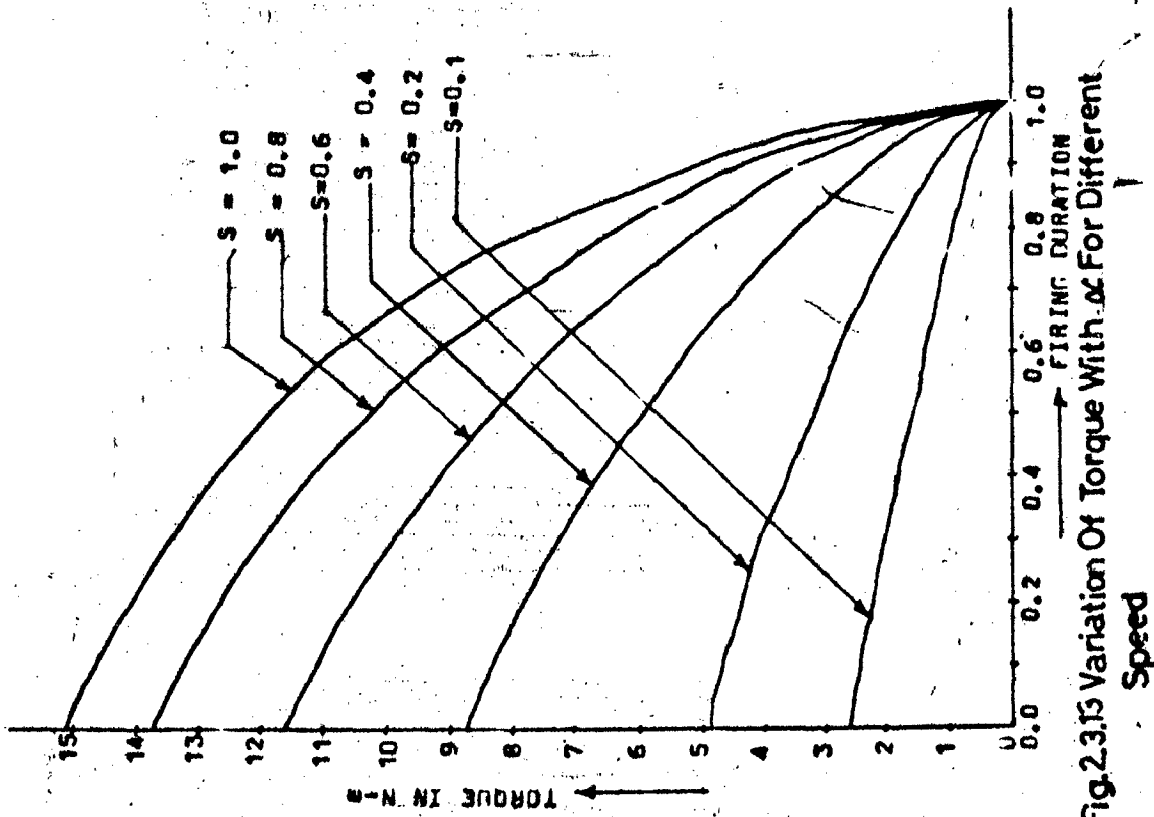


Fig.2.3.15 Variation Of Torque With α For Different Speed

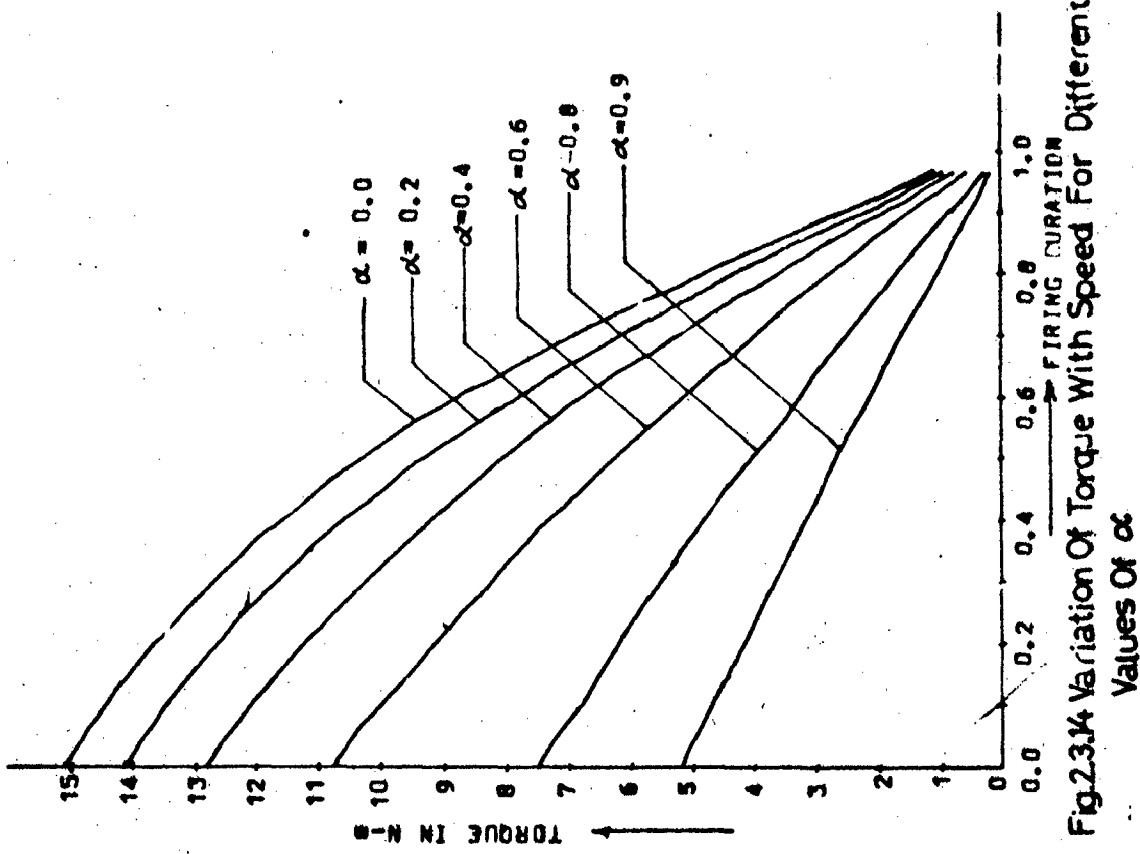


Fig.2.3.14 Variation Of Torque With Speed For Different Values Of α

is the effective torque to drive the mechanical system. The transfer function of the mechanical system may be expressed as follows;

$$G_M(s) = \frac{K_M}{(1+sT_M)} \quad \text{---} \quad (2.3.10)$$

where K_M is the gain constant of the mechanical system, and T_M is the time constant of the mechanical system.

$$K_M = 1/F \quad \text{---} \quad (2.3.11)$$

$$\text{and } T_M = J/F \quad \text{---} \quad (2.3.12)$$

where F is the frictional constant of the rotating system, expressed in N-m/rad/Sec. J is the moment of inertia of the rotating system expressed in Kg - m². Fig.2.3.1 shows the various functional blocks which has been considered for the present study. The various gain and the time constants are given in Table-III., at two different speeds i.e. at 2100rpm and 2400 rpm.

TABLE - IIIVARIOUS GAIN AND TIME CONSTANT USED FOR PERTURBATION
STUDY

$R_s = 9.78$ (Series resistance)
 $R_p = 148.0$ (Parrallel resistance)

Speed	2100 rpm	2400 rpm
K_1	0.0319	0.0319
T_1	0.1	0.1
K_2	14.24 (PI Controller) 60.0 (P Controller)	14.24 (PI Controller) 60.0 (P Controller)
T_2	0.47 (PI Controller)	0.47 (PI Controller)
K_3	- 0.1087	- 0.1087
T_3	0.0055	0.0055
K_4	- 8.333	- 5.12
K_5	- 0.02135	104.72 - 0.0318
K_m	† 104.72	104.72
T_m	16.19	16.19

At 2100 rpm -- $\alpha = 0.85$
 2400 rpm -- $\alpha = 0.72$

C H A P T E R - 3

ANALYSIS OF THE SCHEME- SPEED CONTROL OPERATION

For analysis, a simple Thevenin equivalent circuit of the system has been developed. The effect of Iron losses, stray load losses and losses due to harmonics are neglected. The rotor current I_r , stator current I_s and the developed torque T_d have been developed in terms of the p.u. firing delay (α) and the rotor speed ω_r . These are computed using the standard techniques. Dynamic performance of the system has been studied at two different values of speed. Both P and PI controllers are considered. Analytical results are obtained considering the various functional blocks of Fig.2.3.1. The various differential and algebraic equations which govern the small variations about the operating point are solved using the standard numerical method.

3.1 Theory:

The equivalent circuit diagram of the slip-ring induction motor is given in Fig.3.1.1. The various resistances and ^{reactances} ~~impedances~~ are referred to the stator side. Here V represents per phase supply voltage to the stator of the machine. R_m and jX_m are the magnetising branch components. The parallel combinations of R_m and jX_m gives;

$$R_0 + jX_0 = \frac{R_m \cdot jX_m}{(R_m + jX_m)}$$

$$= \frac{j \cdot R_m \cdot X_m (R_m - j X_m)}{R_m^2 + X_m^2}$$

$$= \frac{R_m \cdot X_m^2}{R_m^2 + X_m^2} + j \cdot \frac{R_m^2 \cdot X_m}{R_m^2 + X_m^2} \quad \text{--- (3.1.1)}$$

Now applying Thevenin's Theorem across points A and B (Fig. 3.1.1). The Thevenin's equivalent model has been obtained (shown in Fig. 3.1.2):

$$E_e = \frac{V_1 (R_0 + j X_0)}{(R_1 + R_0) + j (X_1 + X_0)} \quad \text{--- (3.1.2)}$$

$$\text{and } Z_e = R_e + j X_e = \frac{(R_1 + j X_1) (R_0 + j X_0)}{(R_1 + R_0) + j (X_1 + X_0)} \quad \text{--- (3.1.3)}$$

p.u. firing delay α , has been defined in equation 2.2.1 and for convenience, it is given here;

$$\alpha = \frac{T_{OFF}}{T_{ON} + T_{OFF}}$$

There are two extreme cases for conducting the thyristors;

(a) Thyristors in conducting state;

In the case when thyristors are in conducting state, the equivalent rotor resistance per phase (referred to the stator side) will be as follows;

$$R_t = \frac{1}{S_t} \left[R_2 + \frac{R_p \cdot R_s}{(R_p + R_s)} \right] \quad \text{---} \quad (3.1.4)$$

The value of α will be zero in this case.

(b) Thyristors In Non-conducting State;

In the case when thyristors are in OFF state, the equivalent rotor resistance per phase will be;

$$R_t = \frac{1}{S_r} [R_2 + R_p] \quad \text{---} \quad (3.1.5)$$

In this case the value of α will be unity.

Using equations (3.1.4) and (3.1.5) the equivalent rotor circuit resistance per phase may be expressed generally as follows;

$$R_t = \frac{1}{S_r} \left[R_2 + \frac{R_p \cdot R_s}{(1-\alpha)R_p + R_s} \right] \quad \text{---} \quad (3.1.6)$$

Now the equivalent circuit model considering the effect of solid state resistance controller may be represented as shown in Fig.3.1.3.

Applying Kirchoff's current Theorem for the circuit shown in Fig.3.1.3,

$$\frac{E_g}{I_r} = (R_g + R_t) + j(X_g + X_2)$$

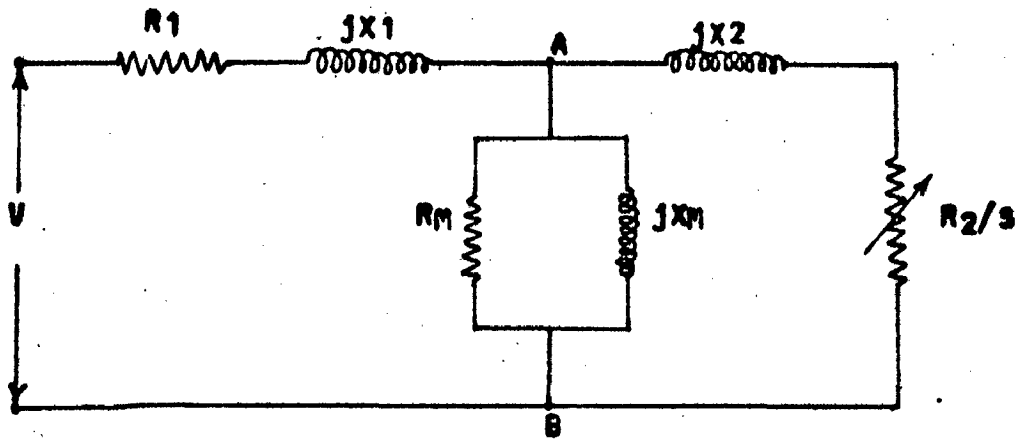


FIG.3.1.1 EQUIVALENT CIRCUIT DIAGRAM OF THE SLIP RING INDUCTION MOTOR.

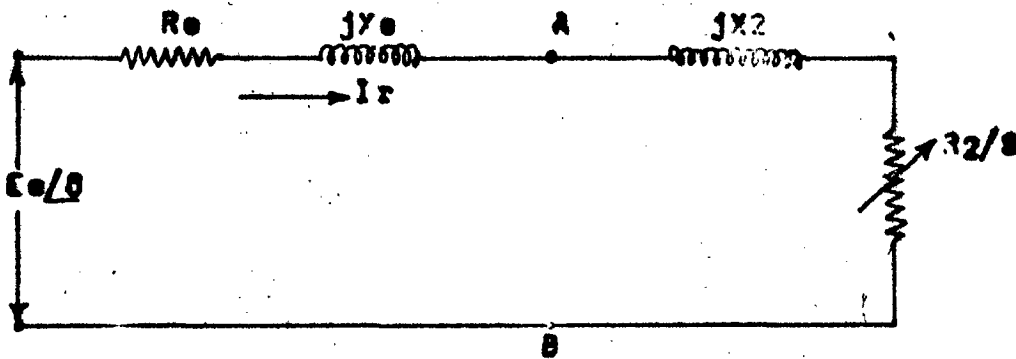


FIG.3.1.2 THEVENIN EQUIVALENT MODEL OF FIG.3.1.1.

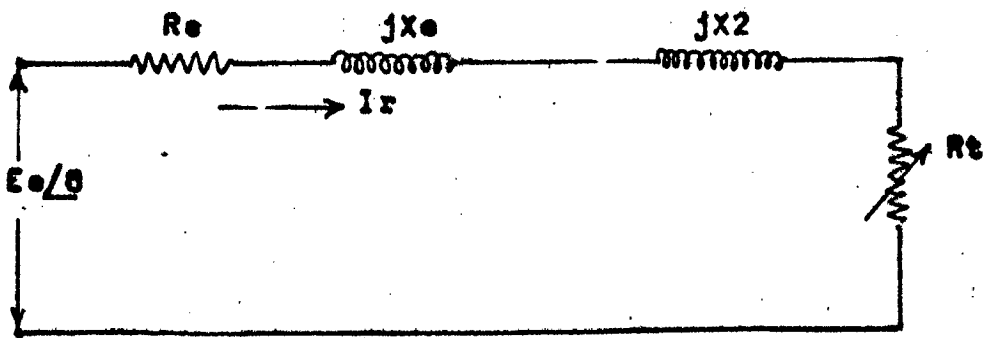


FIG.3.1.3 FINAL EQUIVALENT CIRCUIT MODEL USING THE EFFECT OF SOLID STATE CONTROLLER.

$$= \left[R_e + \frac{1}{S_r} \left[R_2 + \frac{R_p \cdot R_s}{(1-\alpha) R_p + R_s} \right] \right] + j(X_e + X_2)$$

$$\left[\frac{E_g}{I_r} \right]^2 = \left[R_e + \frac{1}{S_r} \left[R_2 + \frac{R_p \cdot R_s}{(1-\alpha) R_p + R_s} \right] \right]^2 + [X_e + X_2]^2 \quad \text{--- (3.1.7)}$$

Rearranging equation (3.1.7) we get;

$$S_r = \frac{\left[R_2 + \frac{R_p \cdot R_s}{(1-\alpha) R_p + R_s} \right]}{\left[\left(\frac{E_g}{I_r} \right)^2 - (X_e + X_2)^2 \right] - R_e} \quad \text{--- (3.1.8)}$$

Also:

$$I_r = \frac{E_g}{(R_e + R_t) + j(X_2 + X_e)}$$

$$= \frac{E_g}{\left[R_e + \frac{1}{S_r} \left[R_2 + \frac{R_p \cdot R_s}{(1-\alpha) R_p + R_s} \right] \right] + j(X_2 + X_e)} \quad \text{--- (3.1.9)}$$

From Fig.3.1.1, the value of I_s may be expressed as follows;

$$I_s = I_r \frac{\sqrt{\left[\left(R_m + \frac{R_2}{S_1} \right)^2 + (X_m + X_2)^2 \right]}}{\sqrt{R_m^2 + X_m^2}} \quad \text{--- (3.1.10)}$$

The torque developed by the machine may be expressed as follows:

$$T_d = \frac{3}{\omega_s} \cdot I_r^2 \cdot R_t \quad \text{---} \quad (3.1.11)$$

Now substituting the values of I_r and R_t from equations (3.1.9) and (3.1.6) respectively into equation (3.1.11) we get:

$$T_d = \frac{3}{\omega_s} \frac{(E_a)^2}{\left[R_a + \frac{1}{s_r} \left(R_2 + \frac{R_p \cdot R_s}{(1-\alpha) R_p + R_s} \right) \right]^2 + (X_2 + X_a)^2} \cdot \frac{1}{s_r} \left[R_2 + \frac{R_p \cdot R_s}{(1-\alpha) (R_p + R_s)} \right] \quad (3.1.12)$$

Using the test machine parameters (Appendix-A) and equations (3.1.9), (3.1.10) and (3.1.12) the rotor current I_r , stator current I_s and the developed torque may be expressed in terms of firing delay α and rotor speed ω_r ($\omega_r = (1-s_r) \omega_s$). Using equation (3.1.12), the variation of torque developed with the firing delay α and the rotor speed ω_r is computed. The curves thus obtained are as follow;

- (a) Torque (V_s) rotor speed for different fixed values of firing delay α . These are shown in Fig. 2.3.13.
- (b) Torque (V_s) firing delay for different fixed values of rotor speed (Slip). These are shown in Fig. 2.3.14.

3.2 Dynamic Performances

The present study investigates the variations of rotor speed due to perturbations in reference voltage and load torque. The various functional blocks are shown in Fig.2.3.1. The different input and output variables of the various blocks are denoted by y_1 , y_2 , y_3 , y_4 , y_5 , y_6 , and y_7 . These variables may be defined as follows:

$$y_1 = \Delta T_d - \Delta T_L \quad \text{---} \quad (3.2.1)$$

(difference between the developed torque and the load torque variations).

$$y_2 = \Delta \omega_r \quad \text{---} \quad (3.2.2)$$

(variation in rotor speed- rad/sec).

$$y_3 = \Delta V \quad \text{---} \quad (3.2.3)$$

(Variation in techogenerator output voltage)

$$y_4 = \Delta V_c \quad \text{---} \quad (3.2.4)$$

(difference between reference voltage variation V_R and y_3)

$$y_5 = \Delta \alpha \quad \text{---} \quad (3.25)$$

(Variation in p.u.firing delay)

$$y_6 = K_4 \cdot \Delta \alpha \quad \text{---} \quad (3.2.6)$$

(Variation of developed torque T_d with small change in with ω_r constant.).

$$y_7 = K_5 \cdot \Delta \omega_r \quad \text{---} \quad (3.2.7)$$

(Variation of T_d with small change in rotor speed ω_r with α constant.).

$$\Delta T_d = y_6 + y_7 \quad \text{---} \quad (3.2.8)$$

These variables are also given in Fig.2.3.1. For the present perturbation study, the differential and algebraic equations which govern the small variations about the operating point are first developed in terms of the above variables. Then these equations are solved simultaneously using standard fourth order Runge-Kutta numerical method. The various differential and algebraic equations are given below. These equations are applicable when PI controller is used;

$$y_1 = y_6 + y_7 - \Delta T_L \quad \text{---} \quad (3.2.9)$$

$$\frac{dy_2}{dt} = \frac{K_M}{T_M} \cdot y_1 - \frac{y_2}{T_M} \quad \text{---} \quad (3.2.10)$$

$$\frac{dy_3}{dt} = \frac{K_T}{T_T} \cdot y_2 - \frac{y_3}{T_T} \quad \text{---} \quad (3.2.11)$$

$$\frac{dy_4}{dt} = \frac{K_C}{T_C} (\Delta V_R - y_3) - K_C \cdot \frac{dy_3}{dt} \quad \text{---} \quad (3.2.12)$$

$$\frac{dy_5}{dt} = \frac{K_F}{T_F} \cdot y_4 - \frac{y_5}{T_F} \quad \text{---} \quad (3.2.13)$$

$$\text{Also } y_6 = K_4 \cdot y_5 \quad \text{---} \quad (3.2.14)$$

$$\text{and } y_7 = K_5 \cdot y_2 \quad \text{---} \quad (3.2.15)$$

When proportional controller is used all the equations (3.2.9) to (3.2.15) are as such, except equation No.(3.2.12). For p controller equation (3.2.12) is replaced by the following equations;

$$y_4 = K_c (\Delta V_R - y_3) \quad \text{---} \quad (3.2.16)$$

$$\text{and } \frac{dy_4}{dt} = -K_c \cdot \frac{dy_3}{dt} \quad \text{--} \quad (3.2.17)$$

Initially, the system is in steady state, therefore, the initial values of the above variables are taken as zero.. The values of various gain and time constants, used for the present dynamic study have been find out and bbe tabulated in Table (III). The above mentioned various algebraic and differential equations are solved by using by using standard numerical methods. The various variables are computed by using standard computer programmes for the fourth order Runge- Kutta method. The flow chart used for the same is given in Fig.3.2.1. Also the developed computer programme for the above is given in Appendix- 'B'.

The dynamic performance is carried out at two different operating points-- one at No.= 2100 rpm, $\alpha_0 = 0.85$ and another one at No = 2400 rpm., $\alpha_0 = 0.72$.

--

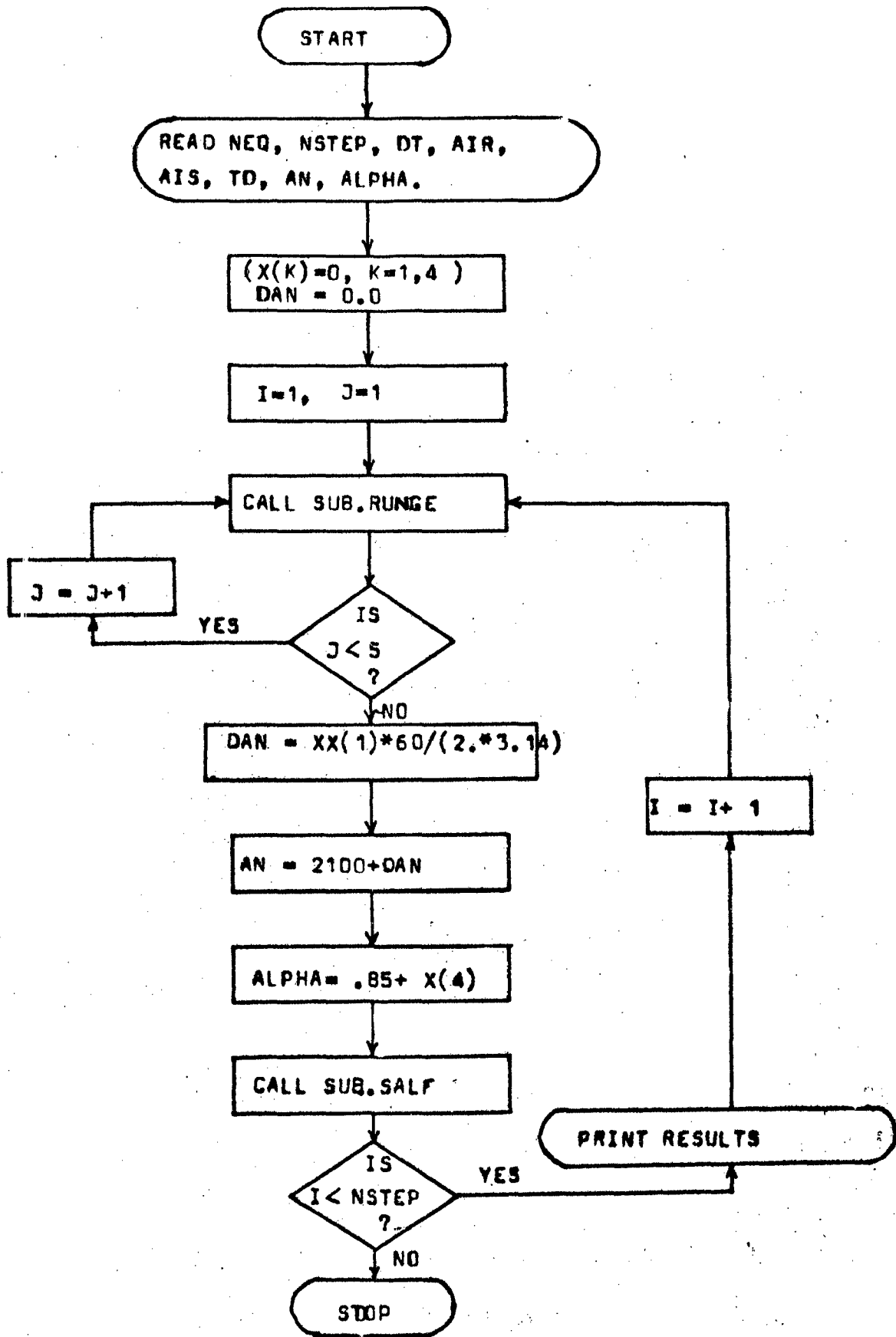


FIG3.2.1(a) MAIN FLOW CHART (to study the dynamic performance for speed control)

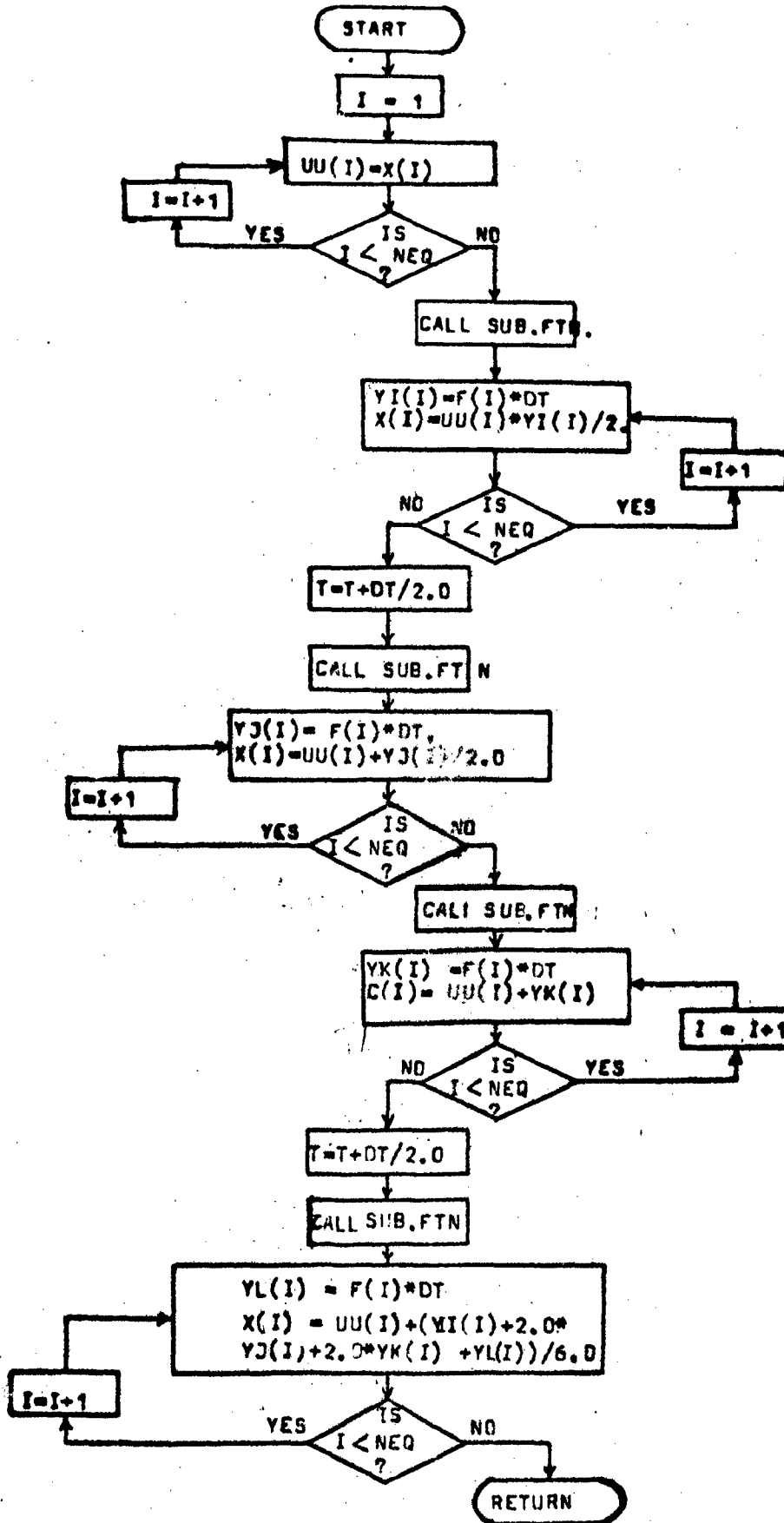


FIG. 3.2.1 (b) FLOW-CHART OF SUBROUTINE RUNGE

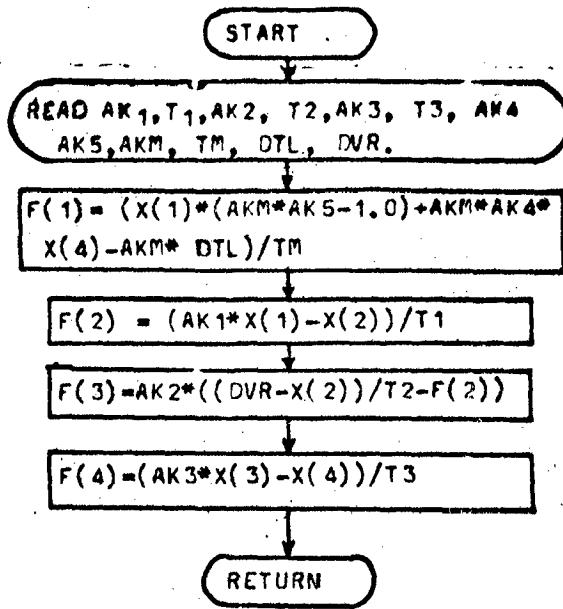


FIG.3.2.1(c) FLOW-CHART OF SUBROUTINE FTN

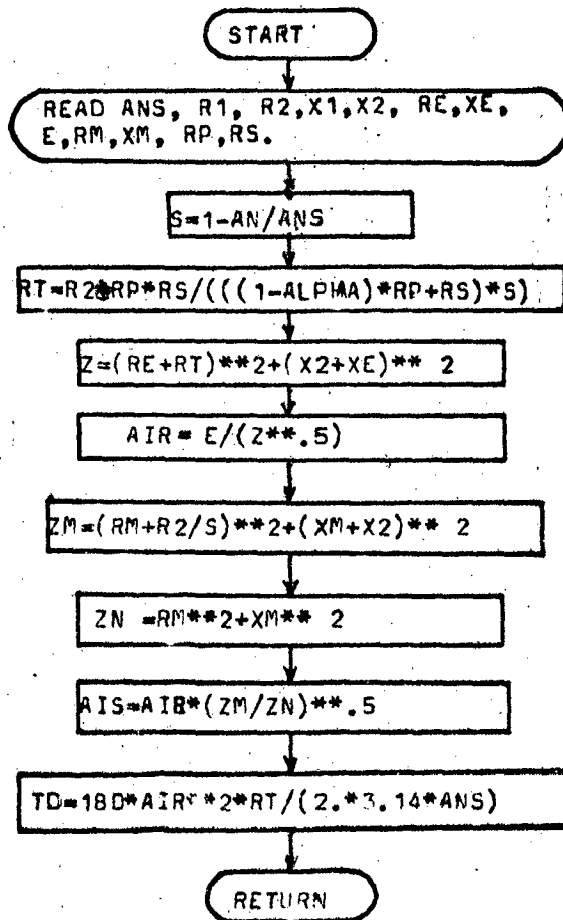


FIG.3.2.1(d) FLOW-CHART OF SUBROUTINE SALE

CHAPTER - 4

ANALYSIS OF THE SCHEME - D.C. DYNAMIC BRAKING

For the dc dynamic braking the stator winding is excited as a field winding. The winding configuration has been choosed as shown in Fig. 4.1. The rotor slip rings are connected to a high resistance bank. Thus, for dc dynamic braking on slip-ring induction motor, the rotor winding works as an armature winding. The two mfs.; both due to armature current and stator direct current, together with their resultant must be referred to a common base; not only in respect of their number of turns but also of the type of current. The equivalent alternating and direct currents produce the equal fundamental mfs., when flowing in a three phase winding.

4.1 Theory:

A simple equivalent circuit configuration of the system including the effect of thyristor controlled external resistance in the rotor circuit has been developed (Fig. 4.1.1). The effect of stray load losses, iron losses and losses due to harmonics and saturation are neglected. The controller has been designed in such a way that the firing delay α becomes a desired function of per unit speed as shown in Fig. 4.1.2.

The stator is excited by the direct current I_d which will produce the same magnitude of fundamental mmf as the alternating

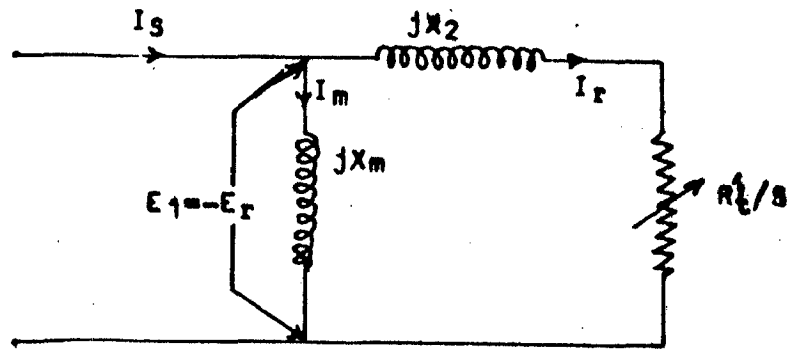


Fig.4.1.1 Per-Phase Equivalent Circuit Under DC Dynamic Braking With Variable Rotor Resistance

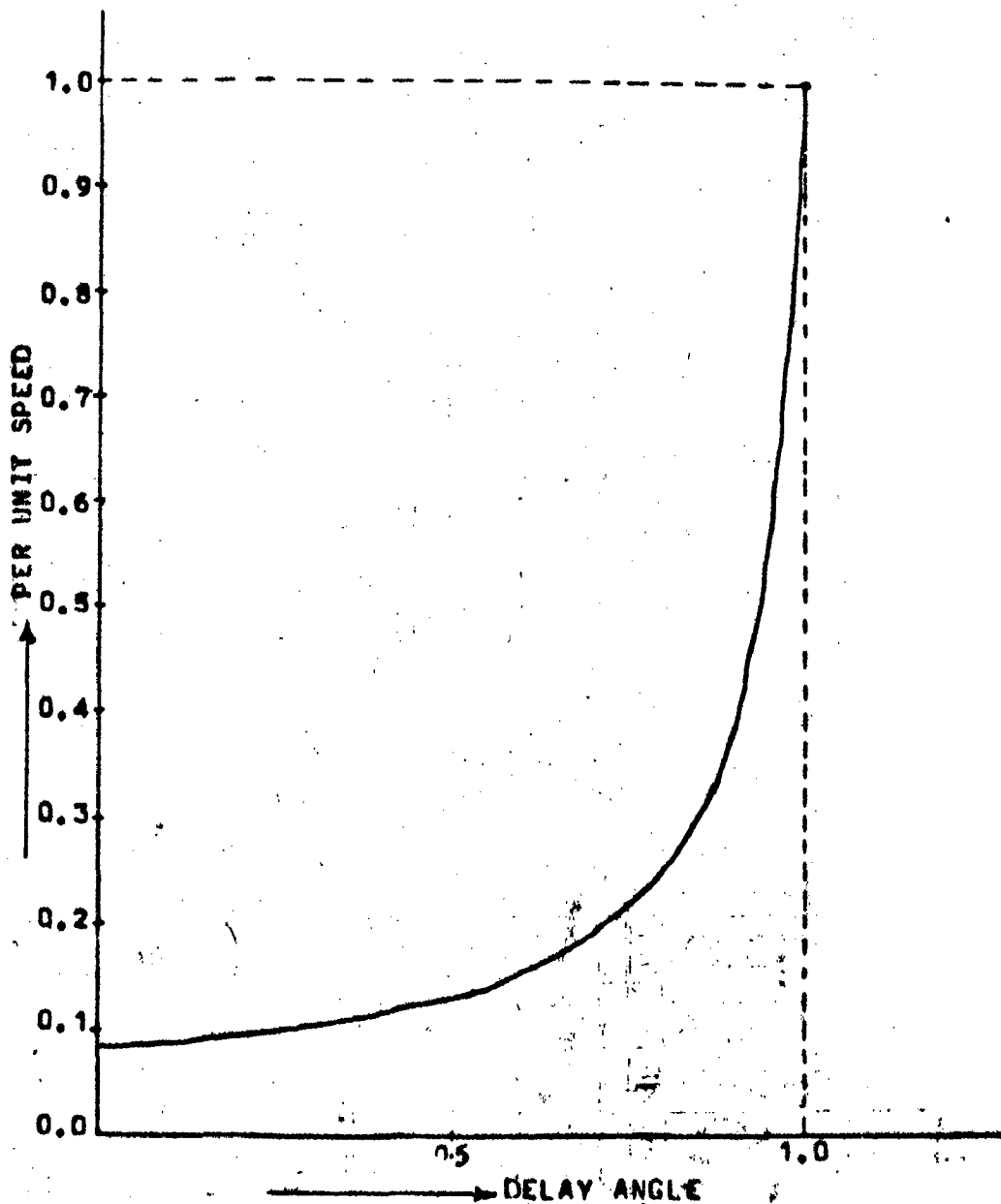


Fig.4.1.2 Variation Of Delay α With Speed

current of magnitude (rms value) as;

$$I_s = \frac{\sqrt{2}}{3} I_d \quad \text{---} \quad (4.1.1)$$

where I_s is the alternating current which is equivalent to the direct current in the stator winding referred to the rotor side.

The field winding is stationary and the relative speed of the rotor (armature) and the field is simply the rotor speed. Speed is taken in place of slip. Here slip is defined as linearly proportional to the rotor speed. Let the armature emf.(air-gap emf.) at synchronous speed is E , the actual emf at any other speed of the rotor, for the same flux will be $S_d.E.$, where ;

$$S_d = \frac{\text{Actual rotor speed}}{\text{Synchronous speed}} \quad \text{---} \quad (4.1.2)$$

An equivalent circuit of the system per phase has been developed. A simple equivalent circuit of the system including the effect of thyristor controlled external resistance is given in Fig.4.1.1. The same firing circuit except some minor changes in controller, has been used for dc dynamic braking also. Here proportional type of controller is used so that the firing delay α becomes a desired function of speed (characteristic curve between p.u.firing delay and rotor speed

given in Fig.4.1.2). From Fig.4.1, it is clear that;

$$I_s = (I_r + I_m) \quad \text{---} \quad (4.1.3)$$

taking the magnitude of each quantity.

$$I_s^2 = I_r^2 + I_m^2 + 2I_r \cdot I_m \cdot \sin \psi_2 \quad \text{---} \quad (4.1.4)$$

where I_r is the rotor current (armature) alternating in nature, and I_m is the resultant alternating current referred to rotor winding. Thus -

$$\begin{aligned} I_r &= \frac{E_{ro} \cdot S_d}{\sqrt{R_{t'}^2 + (X_2 \cdot S_d)^2}} \\ &= \frac{I_m \cdot X_m \cdot S_d}{\sqrt{R_{t'}^2 + (X_2 \cdot S_d)^2}} \quad \text{---} \quad (4.1.5) \end{aligned}$$

where $R_{t'}$ is the equivalent rotor resistance plus external resistance connected in the rotor circuit (referred to rotor side) $R_{t'}$ may be defined as follows;

$$R_{t'} = \left[R_2 + \frac{R_p \cdot R_s}{(1-\alpha) \cdot R_p + R_s} \right] \quad \text{---} \quad (4.1.6)$$

$R_{t'}$, R_p and R_s ; all resistances are referred to rotor side. Also E_{ro} is defined as the referred rotor emf corresponding to the synchronous speed of the machine and ψ_2 is the angle between E_r and I_r .

$$X_m \text{ is the magnetisation reactance} = \frac{E_{ro}}{I_m}$$

Considering equations (4.1.4) and (4.1.5) together, we get the expression for rotor current, .Thus,;

$$I_r = \frac{I_s \cdot X_m}{\left[\left(\frac{R_t'}{S_d} \right)^2 + (X_m + X_2)^2 \right]} \quad \text{---} \quad (4.1.7)$$

The electromagnetic torque developed by the machine may be defined as -

$$T = \frac{3}{\omega_s} \cdot I_r^2 \cdot \frac{R_t'}{S_d} \quad \text{---} \quad (4.1.8)$$

Substituting the values of I_r and R_t' from equations (4.1.7) and (4.1.6) into equation (4.1.8), we get the expression for the developed torque as;

$$T = \frac{3}{\omega_s} \cdot \frac{I_s^2 \cdot X_m^2 \cdot R_t' / S_d}{\left[\left(\frac{R_t'}{S_d} \right)^2 + (X_m + X_2)^2 \right]} \quad \text{---} \quad (4.1.9)$$

The value of R_p is selected in such a manner that the peak braking torque is obtained at the highest possible speed (say synchronous speed N_s), for which;

$$R_t' = X_m + X_2 \quad \text{---} \quad (4.1.10)$$

$$\therefore R_p = (X_m + X_2) - R_2 \quad \text{---} \quad (4.1.11)$$

substituting these condition in equation (4.1.9) the maximum

value of the braking torque will be:-

$$T_{\max} = \frac{3 I_s^2 \cdot X_M^2}{2 \omega_s (X_M + X_2)} \quad \text{--- (4.1.12)}$$

With regard to the value of R_p , the three conditions as studied here:

(a) DC Dynamic Braking with Slip-Ring shorted;

With the slip-ring shorted, the effective rotor resistance per phase will be:

$$R_t' = R_2 \quad \text{--- (4.1.13)}$$

Now putting the value of R_t' from equation (4.1.13) into equations (4.1.7) and (4.1.8) the expressions for rotor current and the braking torque will be as follows;

$$I_r = \frac{I_s \cdot X_M}{\sqrt{\left[\left(\frac{R_2}{S_d} \right)^2 + (X_M + X_2)^2 \right]}} \quad \text{--- (4-1-14)}$$

$$T = \frac{3 I_r^2 \cdot R_2}{\omega_s \cdot S_d} \quad \text{--- (4.1.15)}$$

The condition for maximum braking torque will be that -

$$R_2 = S_{cr} \cdot (X_M + X_2) \quad \text{--- (4-1-16)}$$

where S_{cr} is the slip for which the torque is maximum.

(b) EC Dynamic Braking With Optimum Resistance in the Rotor Circuit;

With an optimum resistance in the rotor circuit, the braking period is improved. Writing equation (4.1.9) for convenience;

$$T = \frac{3I_s^2 \cdot X_m^2 \cdot \frac{R_t'}{S_d'}}{\omega_s \left[\left(\frac{R_t'}{S_d'} \right)^2 + (X_m + X_2)^2 \right]} \quad \text{--- (4.1.9)}$$

The developed torque will be maximum at the slip defined as:

$$S_{cr} = \frac{R_t'}{X_m + X_2} \quad \text{--- (4.1.17)}$$

Putting the value of S_{cr} from equation (4.1.17) into equation (4.1.9) for maximum torque;

$$T_{max} = \frac{3I_s^2 \cdot X_m^2}{2\omega_s (X_m + X_2)} \quad \text{--- (4.1.18)}$$

The braking torque (3) may be defined as follows;

$$T_b = \frac{2 T_{max}}{\frac{S_d}{S_{cr}} + \frac{S_{cr}}{S_d}} \quad \text{--- (4.1.19)}$$

Assuming load torque to be zero;

$$i.e. T_L = 0 \quad \text{--- (4.1.20)}$$

$$\text{Also } T_b = -T \quad \text{---} \quad (4.1.21)$$

Now the dynamic torque equation may be written as;

$$T_d = (T - T_L) = \frac{J d\omega_r}{dt} \quad \text{---} \quad (4.1.22)$$

Where J is the moment of inertia of the rotating system. Putting the conditions from equation (4.1.20) and (4.1.21) into equation (4.1.22).

$$T_d = -T_b = \frac{J d\omega_r}{dt} \quad \text{---} \quad (4.1.23)$$

Considering the equations (4.1.19) and (4.1.23) together:

$$-\frac{2T_{\max}}{\frac{S_d}{S_{Cr}} + \frac{S_{Cr}}{S_d}} = J \frac{d\omega_r}{dt} \quad \text{---} \quad (4.1.24)$$

From equation (4.1.2) it is clear that

$$\omega_r = \omega_s \cdot S_d$$

Differentiating the above equation with respect to t;

$$\frac{d\omega_r}{dt} = \omega_s \cdot \frac{dS_d}{dt} \quad \text{---} \quad (4.1.25)$$

Considering the equations (4.1.24) and (4.1.25) together;

$$\frac{2T_{\max}}{\frac{S_d}{S_{Cr}} + \frac{S_{Cr}}{S_d}} = -J\omega_s \cdot \frac{dS_d}{dt} \quad \text{---} \quad (4.1.26)$$

Rearranging equation (4.1.26); we get;

$$dt = - \frac{J\omega_s}{2T_{max}} \cdot \left[\frac{S_{Cr}}{S_d} + \frac{S_d}{S_{Cr}} \right] dS_d \quad \text{---} \quad (4.1.27)$$

If S_{in} is the initial value of slip the value of slip when braking starts and S_{fin} is the final value of slip. Now taking the integration of both sides of equation (4.1.27);

$$t_{db} = \frac{J\omega_s}{2T_{max}} \int_{S_{fin}}^{S_{in}} \left[\frac{S_{Cr}}{S_d} + \frac{S_d}{S_{Cr}} \right] dS_d \quad \text{---} \quad (4.1.28)$$

$$\text{Assuming } S_{in} = \frac{\omega_r}{\omega_s} = 1.0$$

$$\text{and assuming } S_{fin} = 0.05$$

$$\begin{aligned} t_{db} &= \frac{J\omega_s}{2T_{max}} \left[S_{Cr} \ln S_d + \frac{S_d^2}{2S_{Cr}} \right]_{0.05}^{1.0} \\ &= \frac{J\omega_s}{2T_{max}} \left[S_{Cr} \ln \frac{1.0}{0.05} + \frac{(1.0^2 - 0.05^2)}{2S_{Cr}} \right] \\ &= \frac{J\omega_s}{T_{max}} \left[1.5 S_{Cr} + \frac{0.25}{S_{Cr}} \right] \quad \text{---} \quad (4.1.29) \end{aligned}$$

For getting improved value of t_{db} ;

$$\frac{dt_{db}}{dS_{Cr}} = 0 \quad \text{---} \quad (4.1.30)$$

$$\therefore \frac{J_{ws}}{T_{max}} \left[1.5 - \frac{0.25}{S_{Cr}^2} \right] = 0$$

$$S_{Cr} = 0.408 \quad \text{---} \quad (4.1.31)$$

Therefore the condition for optimum resistance in the rotor may be obtained by putting the value of S_{Cr} from equation(4.1.31) into equation (4.1.17).

$$\begin{aligned} 0.408 &= \frac{R_t'}{X_m + X_2} \\ &= \frac{R_2 + R_p}{X_m + X_2} \end{aligned}$$

$$R_p = 0.408(X_m + X_2) - R_2 \quad \text{---} \quad (4.1.32)$$

Putting the values of R_2 , X_2 and X_m into equation (4.1.32) the value of R_p comes out to be 63.53 Ohm.

(C) DC Dynamic Braking with Solid State Resistance Controller in the Rotor Circuit;

For getting the dc dynamic braking by using Solid State resistance controller, the value of resistance R_p is selected such that the peak braking torque occurs at the highest possible speed (synchronous speed), with thyristors remaining in OFF state. Now as the speed goes down, thyristors start conducting with gradually increased ON time and therefore, the effective rotor resistance gets improved. The reduction in the rotor resistance is

such that the peak braking torque is maintained throughout the speed range. It continues to decrease till the effective rotor resistance becomes marginal at standstill.

Braking with the present solid state resistance controller has been done by selecting the value of R_p by maximising the braking torque at the highest possible speed (synchronous speed) of the rotor, for which -

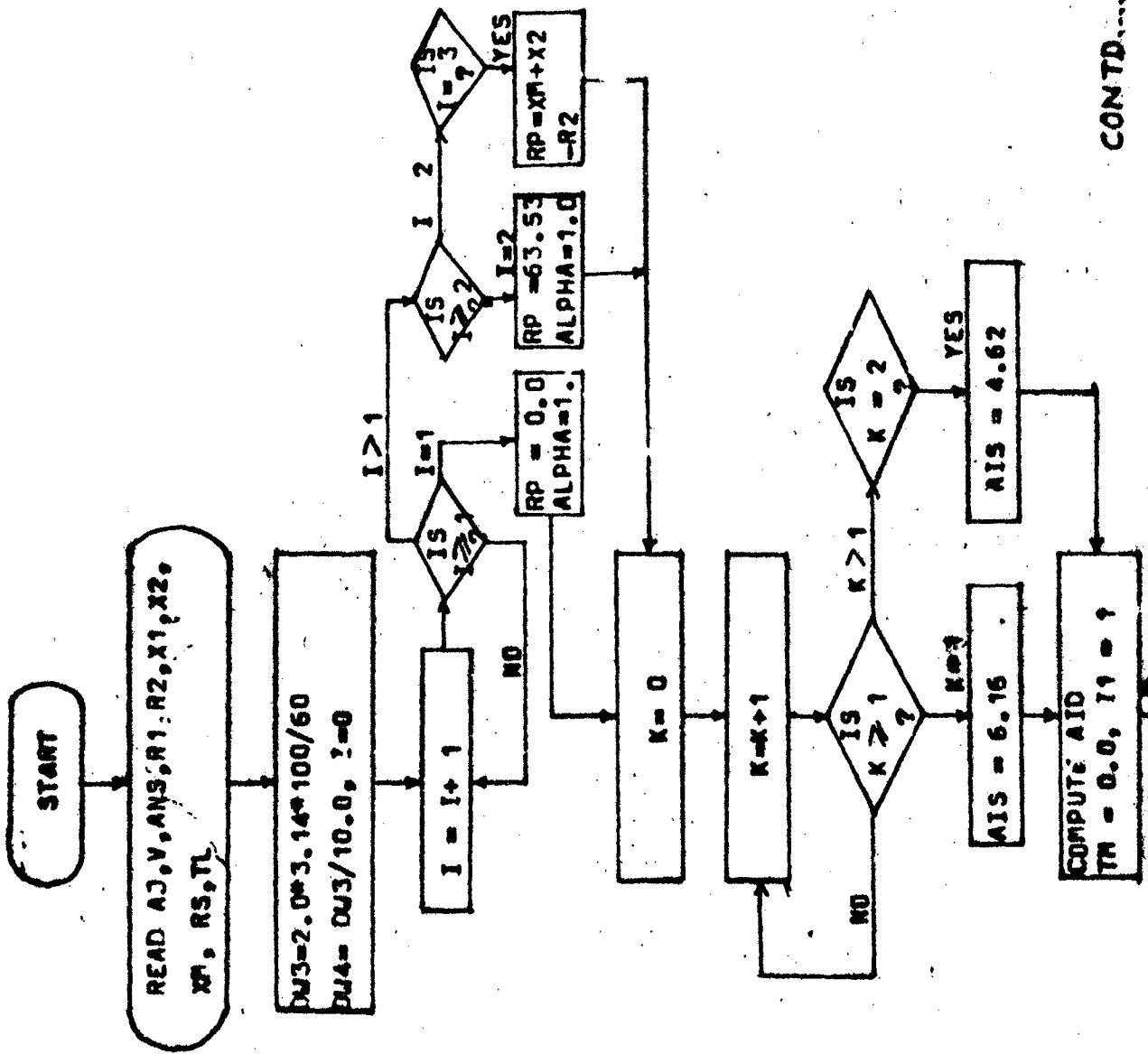
$$s_{cr} = \frac{R_{t^*}}{X_M + X_2} = 1.0 \quad \text{---} \quad (4.1.33)$$

$$R_{t^*} = (X_M + X_2)$$

$$R_p = (X_M + X_2) - R_2 \quad \text{---} \quad (4.1.34)$$

Knowing the values of X_M , X_2 and R_2 , the parallel resistance (external) may be computed with the help of equation (4.1.34). The computed value of R_p comes 161.994 ohm.

The various variables are computed by using standard computer programmes for dc dynamic braking. The flow chart for the above is given in Fig.4.1.3. The dynamic braking has been carried out at two values of stator excitation viz at 0.6 p.u. and 0.8 p.u. of the rated stator current. The developed computer programme for all the three conditions is given in Appendix-'C'.



CONTD....

FIG 4.1.3

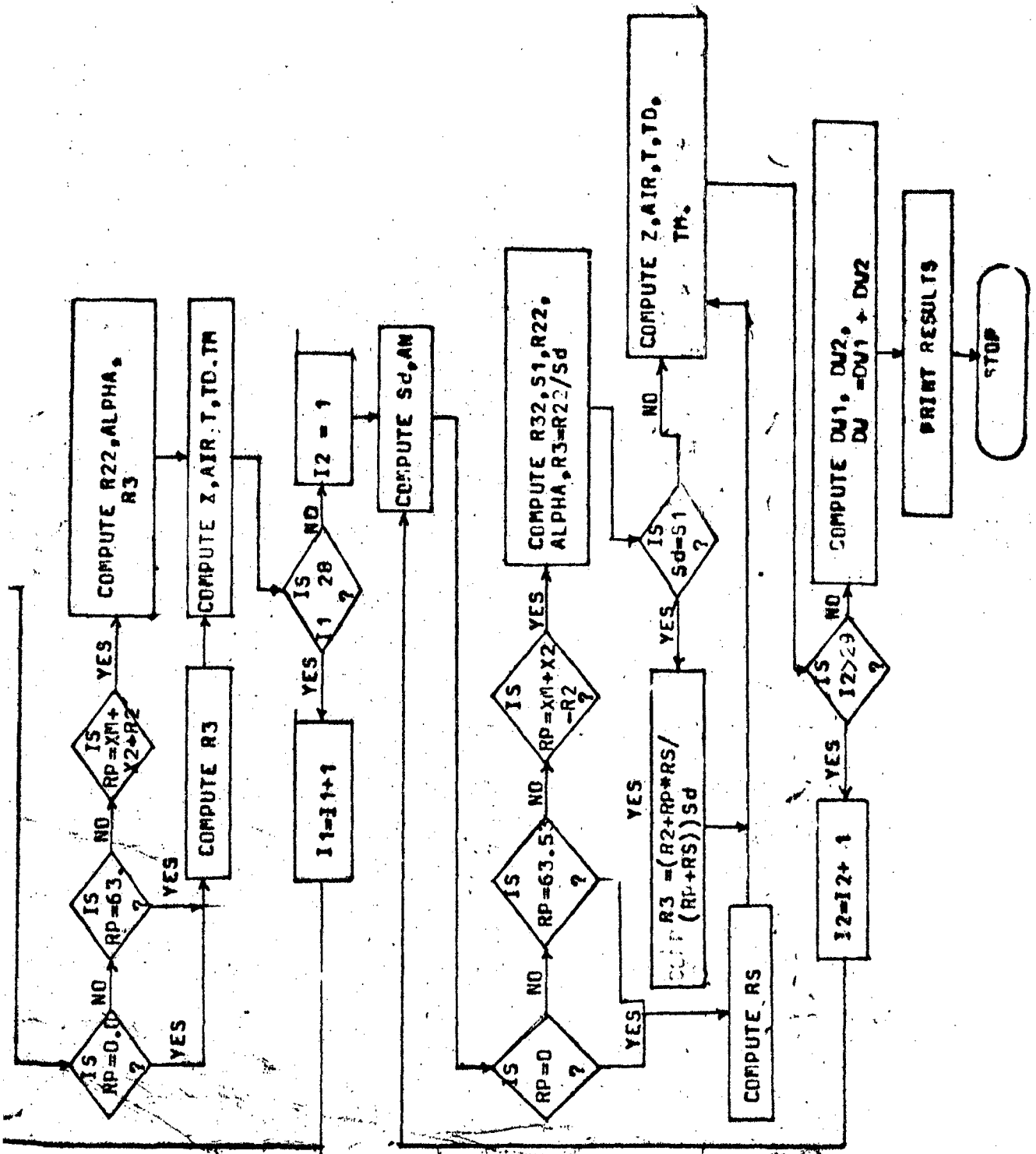


Fig. 4-13. Flow Chart of DC Dynamic Braking

CHAPTER - 5

PERFORMANCE--CHARACTERISTICS

Different performance characteristics both for closed loop speed control and dc dynamic braking are given here. Theoretical and experimental results are compared side by side. For closed loop speed control scheme, the change in rotor speed to sudden changes in reference voltage and load torque have been given. For dc dynamic braking, two different values of stator excitation are taken. All the three conditions; viz., slip ring short-circuited, inserting optimum resistance in the rotor circuit and the solid state resistance controller used in the rotor circuit have been considered. The different machine parameters used are given in Appendix (A).

5.1 Computation of Characteristics and Their Experimental Verification:

For dynamic performance of closed loop speed-control scheme, the differential equations given in Chapter-4, (for proportional and proportional plus integral controllers) are all non-linear in nature. Therefore, the standard numerical method (fourth order Runge-Kutta Method) has been used. The different parameters viz; rotor speed (ω_r), tachogenerator output voltage (V), controller generated signal voltage (V_c), p.u. firing duration (α), the stator current (I_s) and rotor current (I_r) per phase and torque developed (T_d), are com-

puted at different regular intervals of time starting from initial values. The initial conditions are such that the values of Δw_r , ΔV , ΔV_c and $\Delta \alpha$ are zero, for both P and PI controllers. The dynamic equations giving the derivative vector of variables i.e. equations (3.2.10) to (3.2.13) or equations (3.2.10), (3.2.11), (3.2.16), (3.2.17) and (3.2.13) have to be simulated on digital computer. The standard computer programme is obtained for the same. (Appendix-8). The flow charts has been given in Fig.3.2.1. This programme computes and lists the speed of the rotor, p.u.firing delay, stator current perphase (I_s), rotor current per phase and developed torque.

For dc dynamic braking, the performance analysis is governed with the equations given in Chapter-4. Here only proportional controller has been considered. The values of currents, speed, torque time for braking etc..have been computed for flip-ring short circuited, fixed optimum resistance in the rotor circuit and the solid-state resistance controller. The two values of stator excitation are taken for each condition. The different variables given in equations from (3.2.18) to (4.1.34) have to be simulated on digital computer. The computer programme for the same is given in Appendix-9. The flow chart for the same is given in Fig.4.1.3. This programme computes and lists the speed of the rotor, slip, rotor current, braking torque, p.u..firing angle braking time and the total energy losses.

The dynamic performance of the system has been carried out experimentally at the two sets of speed (2100 rpm and 2400 rpm). The response with respect to reference speed has been done for the changes in reference voltage and load torque. The same conditions of reference voltage and load torque have been implied for both P and PI controllers. For dc dynamic braking; the performance has been carried-out for all the three conditions experimentally. Only P controller has been considered here which has slight different parameters than the controller considered for the speed control scheme. The different results both for speed control scheme and dc dynamic braking have been taken with the aid of fast X-Y plotter on the special carbonise sheet. These are discussed in detail in the following paragraphs;

5.1.1 Computed Results;

Performance analysis has been done for getting the results both for speed control scheme and dc dynamic braking. These are given in the following paragraphs;

(a) Speed Control Scheme;

The various gain and time constants used for the perturbation in reference voltage and the load torque are given in Table-III. The analytical results have been obtained with the aid of Computer Programmes given in Sec.5.1..These are given in Fig.5.1.1.

Fig.5.1.1(a) shows the response curves to load perturbation at operating speeds No. = 2100 rpm and 2400 rpm, with while Fig 5.1.1(b) indicates the response curves for PI controller p controller, with other conditions to be same. Fig.5.1.1(c) shows the response curves to reference speed perturbation at both operating speeds No. = 2100 rpm. and 2400 rpm. for P Controller. Fig.5.1.1.(d) shows the response curves with the same operating conditions for PI controller.

(b) DC Dynamic Braking:

The braking characteristics of the test machine have been obtained in terms of rotor speed, braking torque, rotor current per phase and the time taken for braking. These are computed at two different values of stator excitation i.e. at 0.6 and 0.8 p.u. values of the rated values ($I_s = 4.62$ Amp and 6.46 Amp. respectively). All the three conditions of braking viz: with slip-ring shorted, inserting fixed optimum resistance in the rotor circuit and with the solid state resistance controller; are considered separately. Stopping time and the energy losses for the above three conditions are given in Table -IV; because these are considered for the effective braking mode as well as for the heating of the windings.

The braking characteristics of the test machine are obtained in terms of braking torque and rotor current. The relevant curves are shown in Fig.2.1.5 and Fig.5.1.5. Fig(2.1.5) shows the variation of braking torque with speed while the variation

ΔN = CHANGE IN SPEED

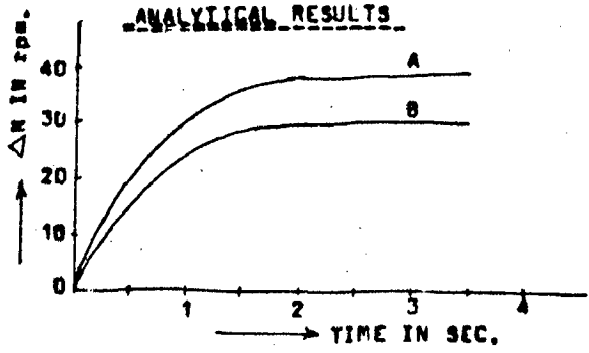


FIG. 5.1.1(a)

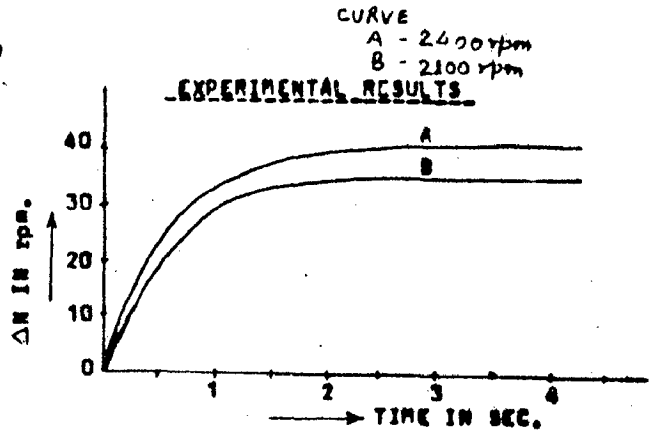


FIG. 5.1.1(b)

RESPONSE TO LOAD PERTURBATION FOR 'P' CONTROLLER

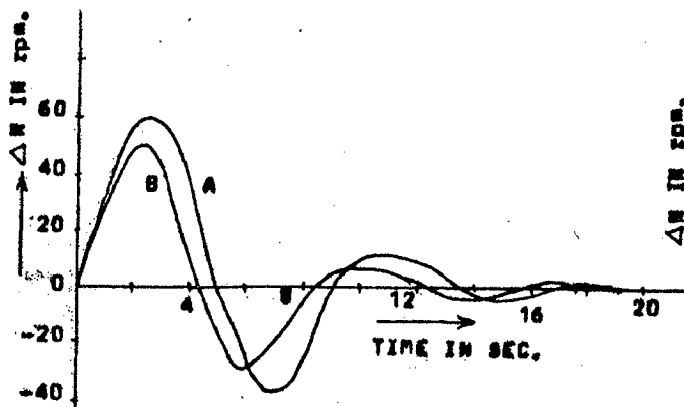


FIG. 5.1.1(b)

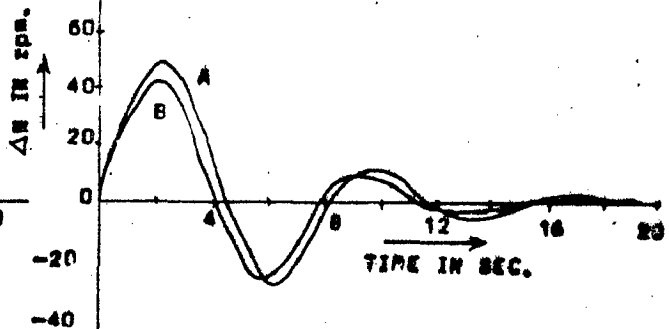


FIG. 5.1.2(b)

RESPONSE TO LOAD PERTURBATION FOR 'PI' CONTROLLER

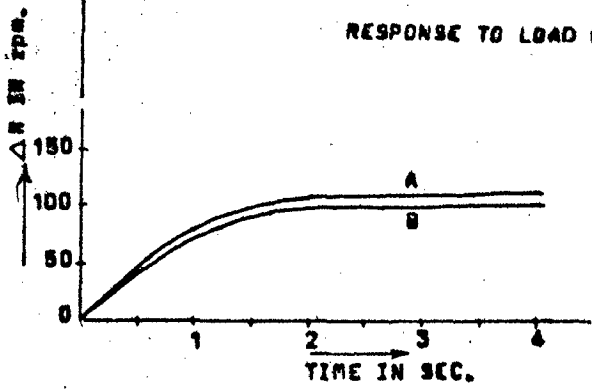


FIG. 5.1.1(c)

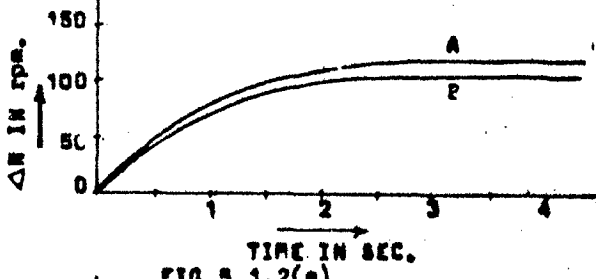


FIG. 5.1.2(c)

RESPONSE TO REFERENCE SPEED PERTURBATION FOR 'P' CONTROLLER.

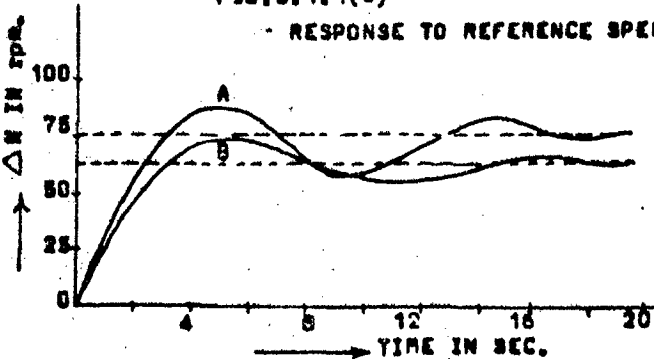


FIG. 5.1.1(d)

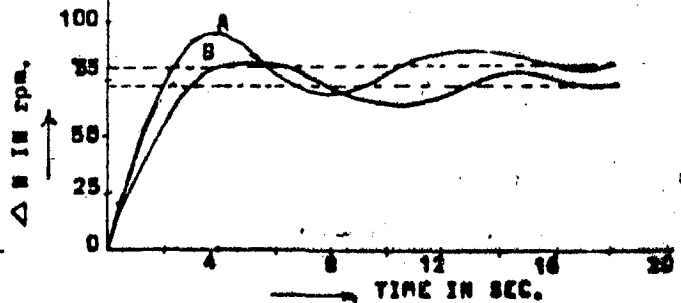


FIG. 5.1.2(d)

RESPONSE TO REFERENCE SPEED PERTURBATION FOR 'PI' CONTROLLER

TABLE - IVSTOPPING TIME AND ENERGY LOSSES IN DC DYNAMIC BRAKING
WITH AND WITHOUT SOLID STATE CONTROLLER

DC EXCITATION 0.6 p.u.				DC EXCITATION 0.8 p.u.		
NAME	STOPPING TIME (Sec.)		ESTIMATED ENERGY LOSS (W-sec)	STOPPING TIME (Sec.)		ESTIMATED ENERGY LOSS (W-sec.)
	CALCULATED	MEASURED		CALCULATED	MEASURED	
STOPPING TIME	12.01	12.4	35120	9.04	9.3	44400
FIXED OPTIMUM RESISTANCE	3.86	3.95	16450	2.43	2.5	17500
SOLID STATE CONTROLLER	2.88	2.8	14210	1.72	1.65	14630

* The natural stopping time of the motor when the supply is disconnected is 56 sec..

<u>CURVE</u>	<u>ROTOR CONDITION</u>
A	• SLIP-RING SHORTED
B	x FIXED OPTIMUM RESISTANCE
C	■ SOLID STATE CONTROLLER

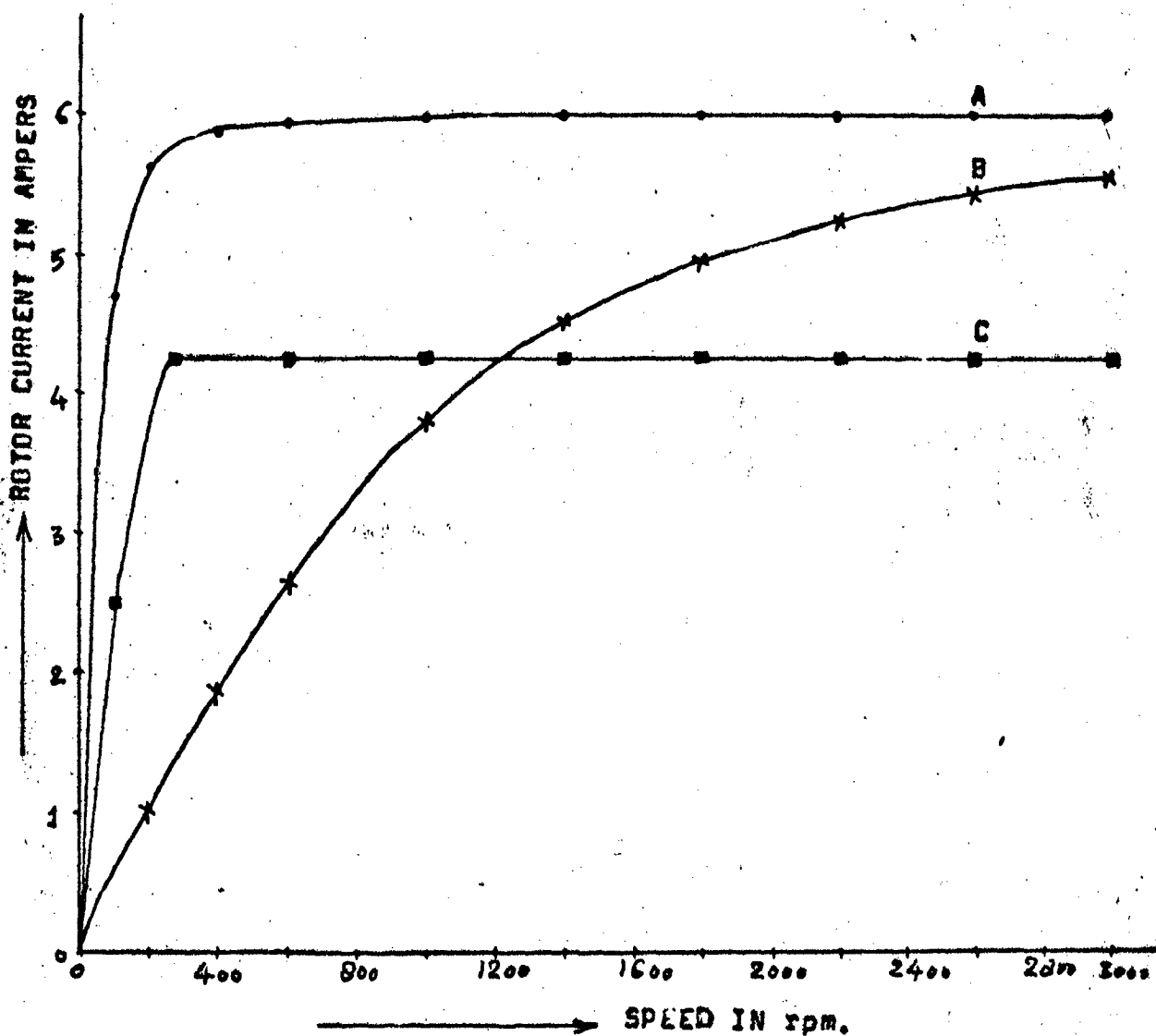


FIG. 5.1.5 VARIATION IN ROTOR CURRENT WITH SPEED FOR SLIP RING SHORTED FIXED OPTIMUM RESISTANCE, AND SOLID STATE RESISTANCE CONTROLLER CASES, $I_s = 0.8$ p.u.

of rotor current with speed is shown in Fig.(5.1.5) curve A represents the performance characteristic for 0.8 p.u. excitation with slip ring shorted condition. Curve B represents the variation for the same excitation with fixed optimum resistance in the rotor circuit. Similarly curve C shows the variation for the case when the solid state resistance controller is in the rotor circuit and the dc excitation is 0.8 p.u..To show the effect of the change in the level of excitation on the braking performance, response for 0.6 p.u. Stator excitation have been computed and the relevant curves for the same are shown in Fig. 5.1.6. Again the variation of braking torque and the rotor current with speed are shown in Figs.5.1.6(a) and 5.1.6(b) respectively.

5.1.2 Experimental Results:

For the ease to compare with theoretical curves, the experimental curves are drawn side by side with the theoretical one. The different curves have been plotted with the aid of fast x-y plotter.

(a) Speed Control Scheme:

The various response curves for reference speed and load torque perturbations are given in Fig.(5.1.2). Fig.5.1.2(a) shown the response curves to load perturbation at operating speeds $N_o = 2100$ rpm and 2400 rpm with P Controller. Fig.5.1.2(b) shows the response curves for PI controller with the same operating conditions. The response curves to ~~the reference~~ the reference

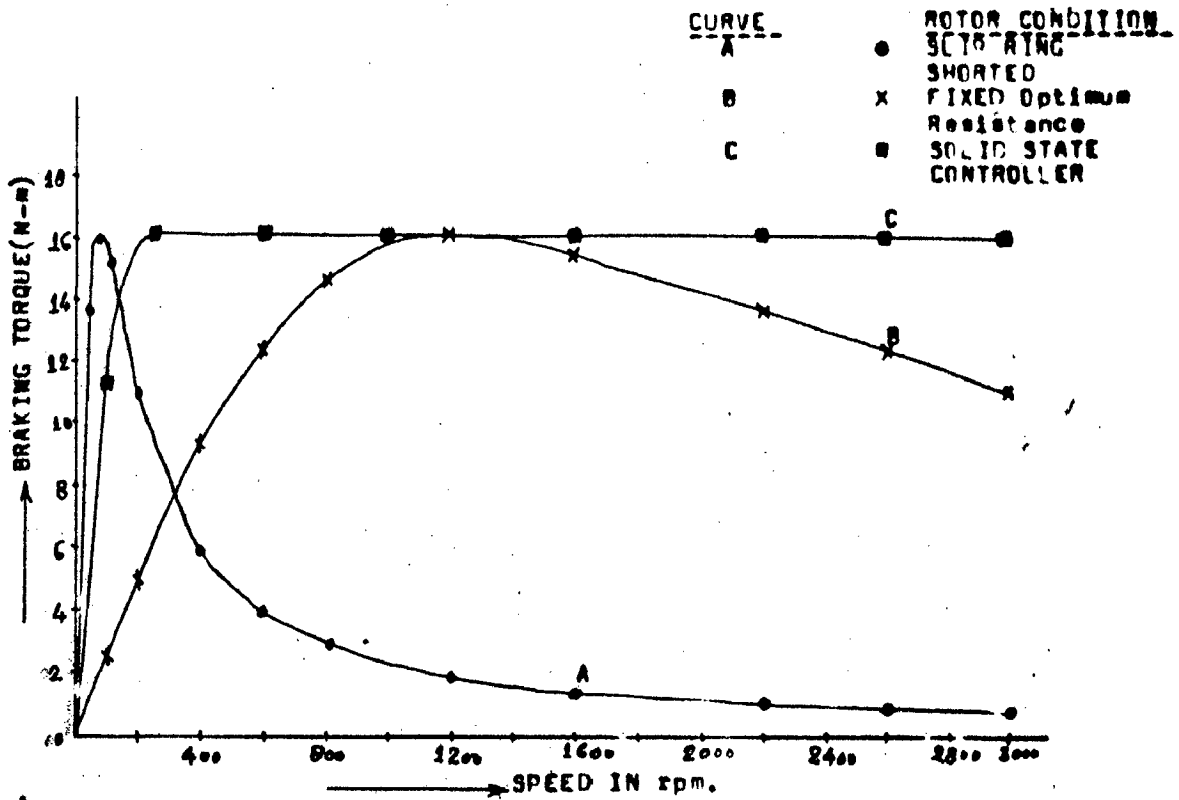


FIG. 5.1.6(a) VARIATION OF BRAKING TORQUE WITH SPEED FOR SLIP-RING SHORTED, FIXED OPTIMUM RESISTANCE AND SOLID-STATE CONTROLLER CASES, $I_s = 0.6$ p.u.

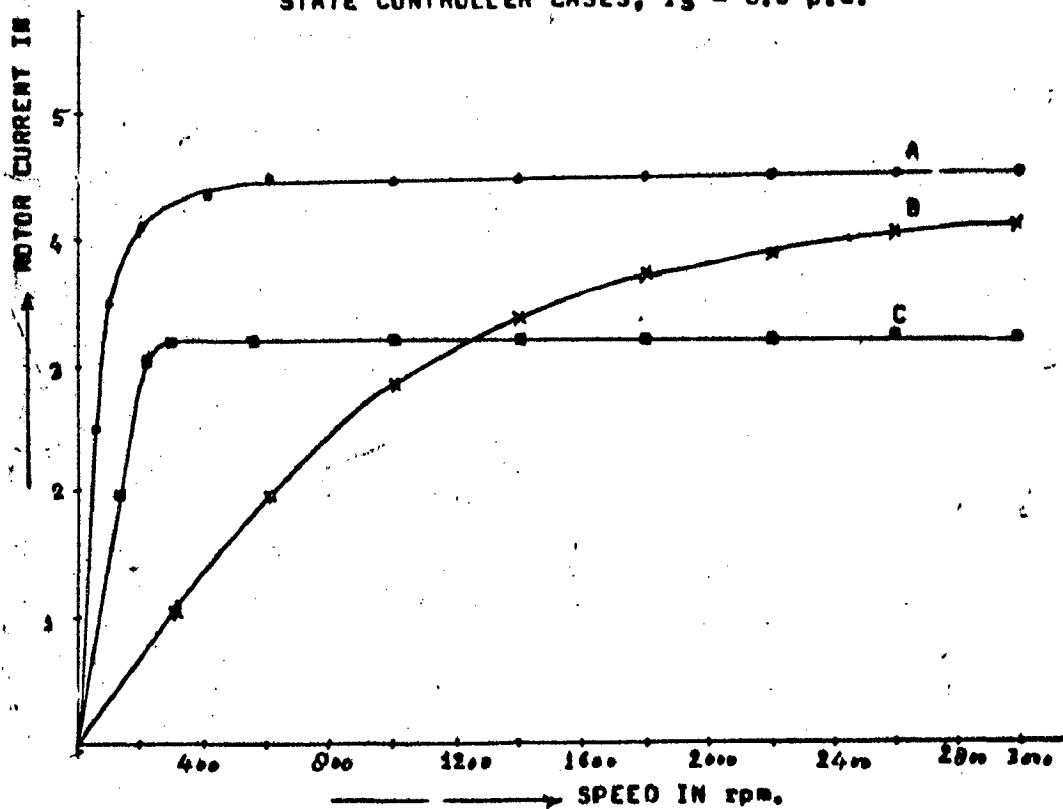


FIG. 5.1.6(b) VARIATION OF ROTOR CURRENT WITH SPEED FOR SLIP RING SHORTED, FIXED OPTIMUM RESISTANCE AND SOLID STATE CONTROLLER CASES, $I_s = 0.6$ p.u.

speed perturbation at both the operating speeds with P controller are given in Fig.5.1.2(c). Fig.5.1.2(d) shows the response curves with the same operating conditions with PI controller.

The variations of stator current with time are given in Fig. 5.1.3 ~~Fig. 5.1.3~~. Fig.5.1.3(a) shows the variation of stator current at 2100 rpm for P controller, while Fig.5.1.3(b) shows the variation of stator current at the same operating speed for PI controller. Similarly at 2400 rpm the variations of stator current for P and PI controller are shown in Fig.5.1.3(c) and Fig.5.1.3(d) respectively.

The effect of load on steady state operating speed has also studied experimentally (Fig.5.1.4). Fig.5.1.4(a) shows the variation of steady state speed (2100 rpm.) with load variations for P and PI controllers. Similar variations in steady state operating speed (2400 rpm) with load variations for both P and PI controllers are shown in Fig.5.1.4(b).

(b) DC Dynamic Braking:

In the braking mode of operation, the variations of rotor speed with time have been plotted with the help of fast x-y plotter. The relevant curves for the same are shown in Fig.5.1.7. Fig.5.1.7(a) shows the variation of speed with time from maximum rotor speed to zero speed for 0.8 p.u. stator excitation with slip -ring shorted. For the same excitation, the variations of

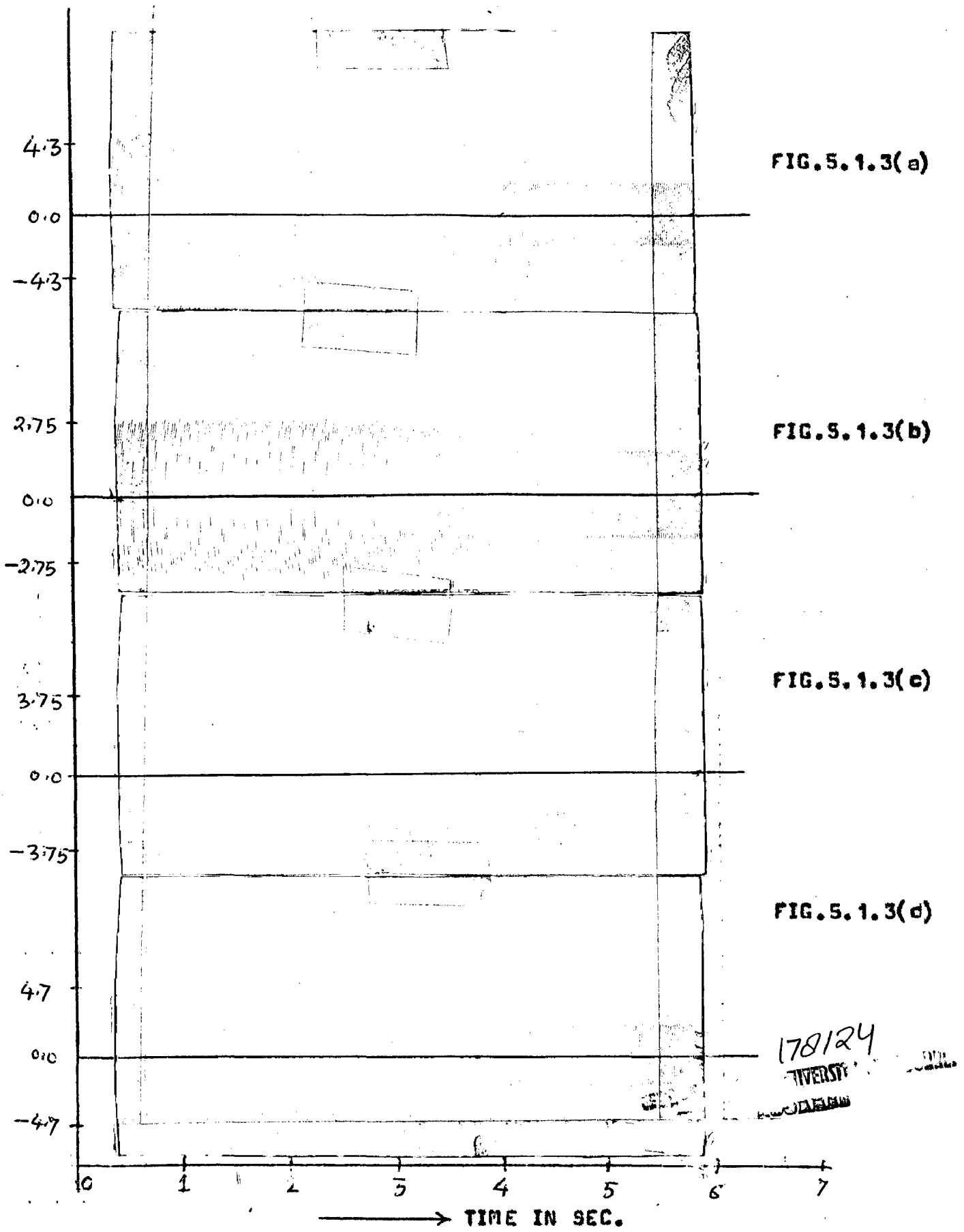


FIG. 5.1.3-VARIATION OF STATOR CURRENT WITH TIME IN CLOSED-LOOP SPEED CONTROL SCHEME (EXPERIMENTAL RESULTS) FOR
(a) P CONTROLLER AT 2100 rpm. (b) PI CONTROLLER AT 2100 rpm (c) P CONTROLLER AT 2100 rpm. (b) PI CONTROLLER AT 2400 rpm.

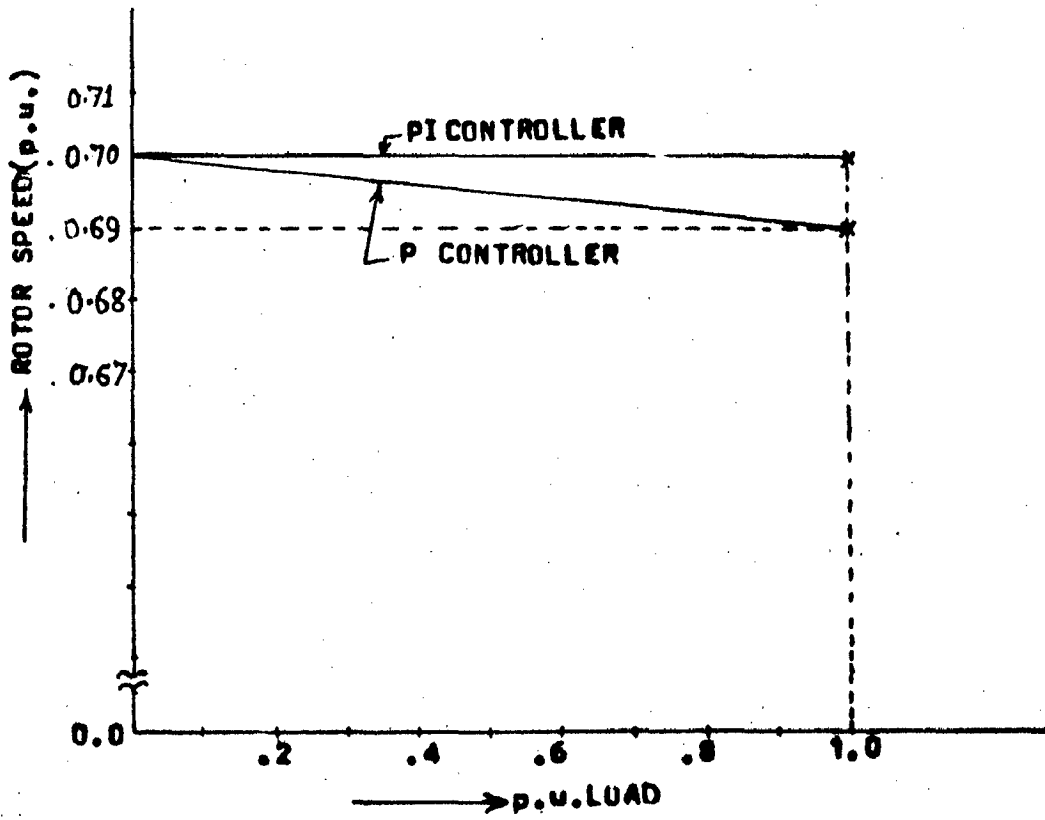


FIG. 5.1.4(a)

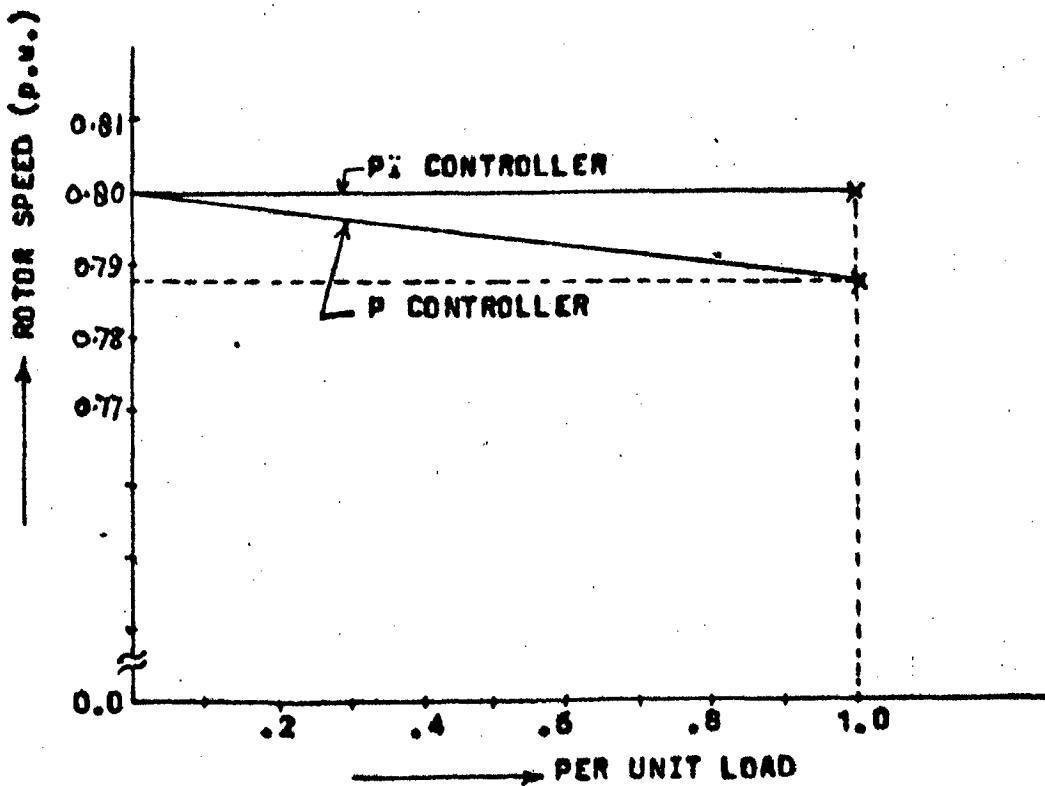


FIG. 5.1.4(b)

FIG. 5.1.4- VARIATION OF STEADY STATE OPERATING SPEED WITH VARIATION OF LOAD TORQUE AT (a) 2100 rpm and (b) 2400 rpm.

speed with time for fixed optimum resistance in the rotor circuit and for solid state resistance controller (P) are shown in Fig.5.1.7(b) and Fig.5.1.7(c) respectively. Similarly, the variations in the rotor speed with braking time for 0.6 p.u. stator excitation, with rotor shorted, fixed optimum resistance in the rotor circuit and with the solid state resistance controller are shown in Figs.5.1.8(a), 5.1.8(b) and 5.1.8(c) respectively.

5.2 Discussion of Results:

In speed control the perturbation studies have been carried out at the two different operating speeds - one at 2100 rpm., $\alpha_0 = 0.85$ and the another one at 2400 rpm., $\alpha_0 = 0.72$. The analytical as well as experimental results are given in Figs.5.1.1 and 5.1.2. Comparing the experimental observations with the analytical results, the following observations are made;

- (i) For load perturbation, the system reaches to steady state much faster using P controller than with PI controller.
- (ii) For the same load disturbances, P controller introduces a small variation in the steady state speed while the steady state error is negligible with PI controller.
- (iii) For the reference voltage perturbation, the system reaches to new steady state value of speed much faster using P controller while PI controller is slower. Also for the same variation in reference voltage, P controller introduces some error with respect to new value of speed. There is negligible error using PI controller.

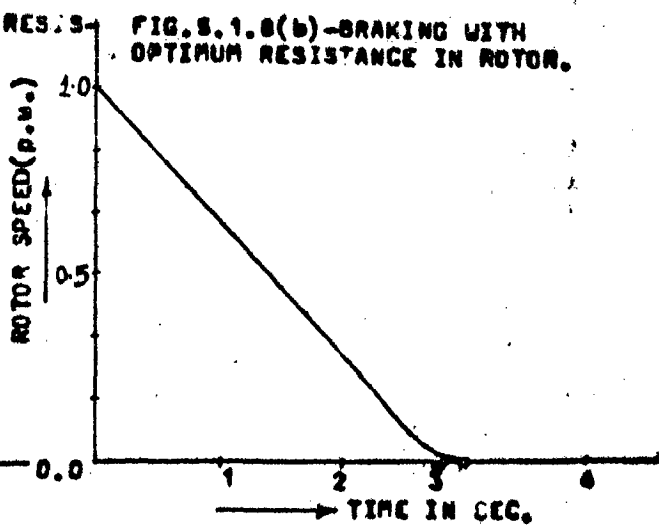
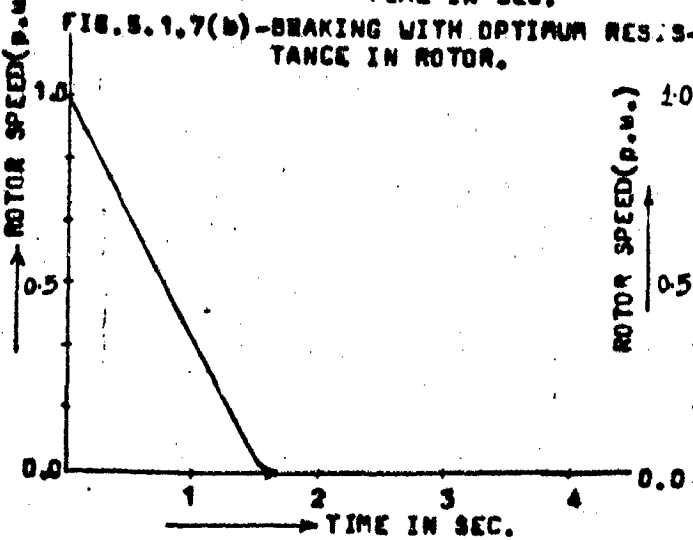
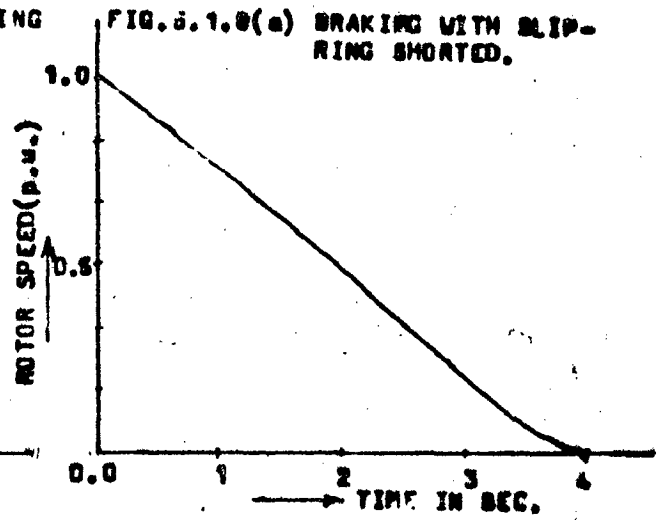
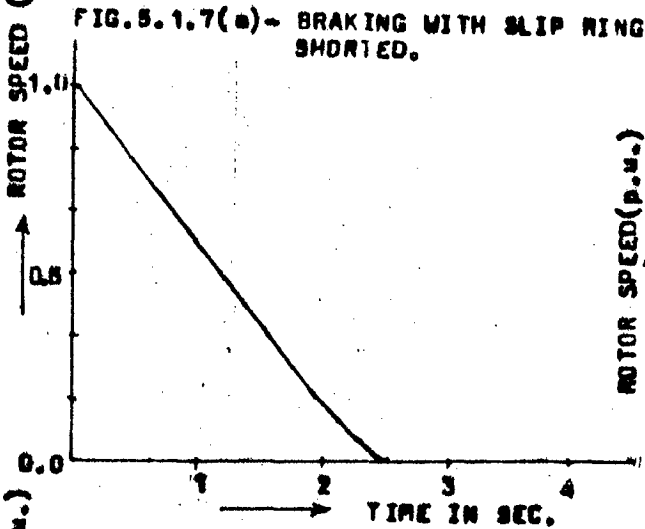
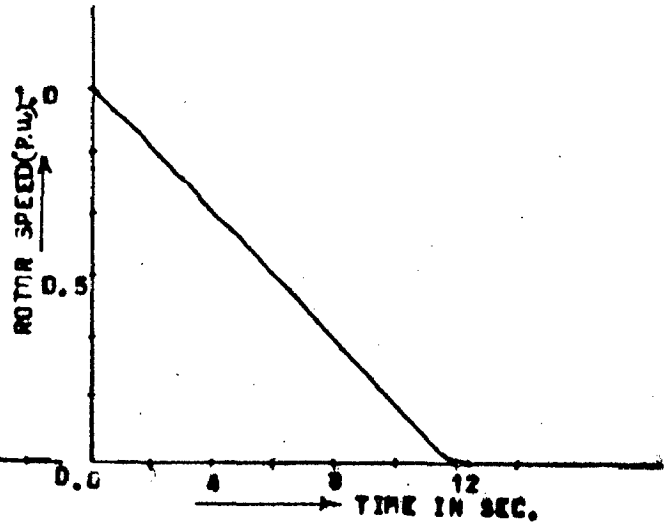
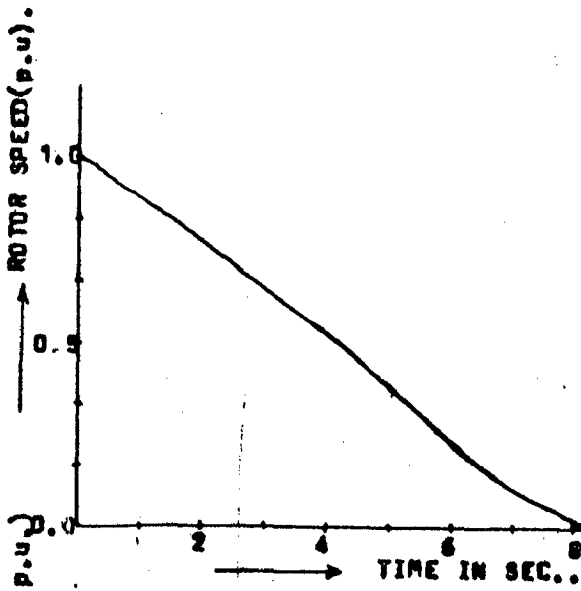


FIG. S.1.7(a) - BRAKING WITH SLIP RING SHORTED. FIG. S.1.8(a) - BRAKING WITH SLIP RING SHORTED.

FIG. S.1.7(b) - BRAKING WITH OPTIMUM RESISTANCE IN ROTOR. FIG. S.1.8(b) - BRAKING WITH OPTIMUM RESISTANCE IN ROTOR.

FIG. S.1.7(c) - BRAKING WITH SOLID STATE CONTROLLER. FIG. S.1.8(c) - BRAKING WITH SOLID STATE CONTROLLER.

(EXPERIMENTAL RESULTS) VARIATIONS OF ROTOR SPEED WITH TIME FOR DC DYNAMIC BRAKING (S.1.7) .8 p.u. EXCITATION (S.1.8) .6 p.u. EXCITATION

- iv) There is a slight difference between the analytical and experimental results.

For dc dynamic braking, the effectiveness of the braking using solid state resistance controller may be seen than with the slip-ring shorted as well as with the fixed optimum resistance in the rotor circuit. From the curves given in Figs.(5.1.3) (5.1.4), (5.1.5) and (5.1.6) and Table IV, the following observations are made:

- (i) With solid state resistance controller in the rotor circuit, the braking torque remains at peak level throughout the speed range and therefore, the braking action is much faster than with slip-ring shorted and optimum resistance in the rotor circuit condition. The stopping time thus obtained is the optimum for a particular excitation.
- (ii) The energy losses in both stator and rotor windings are minimum with solid state resistance controller than with the other two conditions.
- (iii) There is no jerky effect with solid state controller, while much jerks are observed for the other two conditions. Much variations in braking torque are observed for slip-ring shorted and optimum resistance conditions.
- (iv) The stopping time is reduced with the increase in dc excitation. This can be seen from Figs.(2.1.5), (5.1.5) and (5.1.6).

CHAPTER - 6CONCLUSIONS AND SUGGESTIONS FOR FURTHER WORK

The closed-loop solid state resistance controller for the slip ring induction motor (the test machine) has been designed, fabricated and tested. The functional block-diagram with various transfer functions has been given in detail. The main parts of firing control scheme have been designed and fabricated. The firing control circuit is so designed that it becomes simple, economical, and requires less space. The variation of speed for the fixed value of load torque has been obtained by varying the rotor resistance continuously between R_{ON} and R_{OFF} in closed loop manner. The performance characteristics for the speed control scheme have been given analytically and experimentally. Both P and PI controllers have been considered. It is observed that the change in operating speed due to load perturbation for PI controller is negligible while with P controller it is around 2%.

The same solid state resistance controller for dc dynamic braking has been developed. P controller for the firing control scheme is considered. The variations of braking torque, rotor current with rotor speed and the energy losses have been studied theoretically for all the three conditions viz..with the slip-ring shorted, with optimum resistance in the rotor and with the solid state resistance controller. The braking time has been

compared for all the three conditions and observed that the braking time with optimum resistance is better than with slip-ring shorted condition. It is further observed that the braking time with solid state resistance controller is much better than with optimum resistance in the rotor circuit. Both analytical and experimental results have been compared and found a very small variation in between. The braking has been done at two different values of dc excitation. It is also observed that the energy losses are minimum with the solid state resistance controller.

Thus the control circuitary used here for closed loop speed control scheme and dc dynamic braking is much simpler and economical in comparison to other solid state resistance control schemes i.e. phase controlled and chopper controlled schemes.

Further, in this scheme, some changes may be done to reduce the space and the cost of the scheme. This scheme may be used in industries to control the speed of the drives as well as to perform effective braking in certain applications. The scheme is economical for medium size of machines. Further study for the variation of stator current, rotor current with load torque can be performed. The effect of harmonics developed due to sudden ON and OFF operation of thyristors can also be performed. In case

of dc dynamic braking, the experimental results for the variations of load torque and the rotor current can be obtained. Saturation can be considered for further accurate analysis, complete control circuit for both the schemes can be developed jointly for field applications.

-- *** --

B I B L I O G R A P H Y

- 1) Arockiasamy R. and S. Dorai Pandey., " A Novel Trigger Scheme for sustained Triggering of SCR," IEEE Trans. Vol. IECI-22, No. 2., May 1975, PA 233-235.
- 2) Basu, R.P., " Variable Speed Induction Motor Using Thyristors in the Secondary Circuit.," IEEE Trans., Vol. PAS-90, March-April 1971, AP-509-514.
- 3) Chilkin, M., " Electric Drives ", Mir Publishers, Moscow 1976.
- 4) Dubey, G.K. and G.C. De., " DC Dynamic Braking of Induction Motor with Saturistors in its Rotor Circuit.," IEE Proceedings, ~~of the~~ Vol. 118., No. 11, 1971, PP-1585.
- 5) Dubey, G.K. and P.R. Joshi, "Optimum dc Dynamic Braking Control of an Induction Motor Using Thyristor Chopper Controlled Resistance," IEEE Trans., Vol. IECI-21, No. 2, 1974 PP-60.
- 6) Gupta J.R.P., ~~and~~ B. Singh and B.P. Singh, " Improved Method of DC Dynamic Braking of Wound Rotor Induction Motor." IE(I) Journal- ~~1~~, Vol.-64, October 1983, pp-95-99.
- 7) Gallagher P.J. and W. Shepherd., "Operation of Two Parallel connected Thyristor controlled resistive Loads with Integral Cycle Triggering, "IEEE Trans., On IECI, November 1975., pp-510.
- 8) G. E. C. SCR Manual.
- 9) Krishnan T. and B. Ramaswami, " A Fast Response DC Motor Speed Control System, "IEEE Trans., Vol. IA-10, No. 5., Sept./October 1974, pp-643-651.

- 10) Langsdorf, A.S., "Theory of Alternating Current Machinery", Tata McGraw-Hill Publishing Company, Ltd., New Delhi 1974.
- 11) Parish E.A. Jr., and E.S. Mc Voy., "A Theoretical Model for Single Phase Silicon Controlled Rectifier System," IEEE Trans., Automatic Control., pp-577- 579, Oct., 1967.
- 12) Ramamoorthy, M. "Introduction to Thyristors and their Applications.," Affiliated East- West Press Pvt. Ltd., 1977..
- 13) Ramamoorthy, M. and M. Arunachalam, "A Solid State Controller for Slip-ring Induction Motor," IEEE Annual Meeting on Industry Applications., 1977.
- 14) Ramamoorthy, M. and M. Arunachalam, "Dynamic Performance of a Closed Loop Induction Motor Speed Control System with Phase-controlled SCR's in the Rotor," IEEE Trans. Vol. IA-15 No. 5, Sept./October 1979., pp489- 493.
- 15) Ramamoorthy M. and M. Arunachalam, "Solid State Speed Control of Slip-ring Induction Motors," Presented at the 1977 Midwest Power Symposium.
- 16) Rao, S.S., "The Finite Element Method in Engineering," Publisher; Robert Maxwell, M.C.,
- 17) Say, M.G. "The Performance and Design of Alternating Current Machines," S.I. Pitman & Sons Ltd. London.
- 18) Sen, P.C. and K.H.J. Ma., "Rotor Chopper Control for Induction Motor Drive," IEEE Trans., Vol. IA -77, Jan.-Feb. 1975, pp43- 49.,
- 19) Srinivasan, P.S., C. Velayudhan and P.K. Charlu, "A Solid State resistance Controller for 3 Phase Slip ring Induction Motor," Electric Machines and Electromechanics, Vol. 6, No. 2., March- April 1981., pp153- 156.

- 20) Wani, N.S. and M.Ramamoorthy., "Chopper Controlled Slip Ring Induction Motor, " IEEE Trans., Vol.IECI-24., May 1977, pp.153- 161.

--

APPENDIX - 'A'SPECIFICATIONS AND PARAMETERS OF THE TEST MACHINEName Plate Details of Generalised
Electrical Machine:

Make	-	Mawdsley's Ltd., England
Stator	-	200/240V, Δ connected, 15 A.
H.P.	-	3.0
Phase	-	3
Poles	-	2
Cycles	-	50/60
RPM	-	2860
Insulation	-	Class 'E'
Rotor	-	Δ connected
Turns ratio	-	3
Moment of Inertia (J)	-	0.1546 Kg m^2
Frictional constant (F)	-	0.0095N-m/rad/sec.

Other Electrical Parameters:

E	=	191.7 Volt
R ₁	=	2.75 Ohm.
R ₂	=	4.33 Ohm.
X ₁	=	3.924 Ohm.
X ₂	=	3.924 Ohm.
R _G	=	2.63 Ohm.
R _M	=	305.0 Ohm.
X _E	=	5.06 Ohm.
X _M	=	162.4 Ohm.
R _O	=	63.83 Ohm
X _O	=	121.66 Ohm
R _S	=	9.78 Ohm.
R _P	=	148.0 Ohm.

++++*****

CL. 12/11
MCP
111